

Narve Nikolai Opsahl

Expression profiles and initial RNAi experiments with tyrosine hydroxylase and tryptophan 2,3-dioxygenase encoding genes in the salmon louse (*Lepeophtheirus salmonis*)

Master's thesis in Biology

Supervisor: Atle M. Bones

Co-supervisor: Prashanna Guragain

June 2021

Narve Nikolai Opsahl

Expression profiles and initial RNAi experiments with tyrosine hydroxylase and tryptophan 2,3-dioxygenase encoding genes in the salmon louse (*Lepeophtheirus salmonis*)

Master's thesis in Biology
Supervisor: Atle M. Bones
Co-supervisor: Prashanna Guragain
June 2021

Norwegian University of Science and Technology
Faculty of Natural Sciences
Department of Biology



Abstract

The salmon louse is an ectoparasite copepod on salmonids. It causes substantial economic loss in the salmon industry and represents a welfare threat to farmed salmonids and a potential threat to the sustainability of several wild salmonid populations. Experimental post-transcriptional knockdown of specific genes by RNA interference (RNAi) is a method used to characterize the function of genes in many organisms, including the salmon louse, and experimental RNAi have been achieved in several of the salmon louse's developmental stages. RNAi, in combination with other techniques and methods, might expand the understanding of parasite-host interactions, as well as help identify molecular targets for novel chemical treatments and vaccine antigens.

In this project, the two genes *LsPale* and *LsTDO* in the salmon louse, encoding tyrosine hydroxylase (TH) and tryptophan 2,3-dioxygenase (TDO), respectively, were studied. The two enzymes represent key steps in the metabolism of several neurotransmitters, pigments, and other metabolites of tyrosine and tryptophan. Phylogenetic analysis revealed that both genes belong to their arthropod gene families and are closely related to corresponding copepod genes. Further, the two genes were knocked down by RNAi in the salmon louse nauplii stages. A successful knockdown was only obtained for *LsPale*, and the knockdown was detectable for less than seven days. No morphological or behavioral changes were observed at three or seven days after treatment, but larvae were inactive immediately after double-stranded RNA (dsRNA) delivery. Expression profiling of the two genes revealed that the expression of *LsPale* is strongly increased before and through the metamorphic molt to copepodite and that *LsTDO* is expressed in both the planktonic and the parasitic stages of the salmon louse, with a peak in preadult and adults.

As the results presented here indicate that the genes are involved in important developmental phases in the life cycle of the salmon louse, more work should be conducted to characterize the function of the two genes. It is also suggested that *LsTDO* might play a role in eye pigmentation, and therefore could serve as a suitable selection marker when developing CRISPR/Cas9-based genome editing method for salmon louse. Further, the project illustrates that, despite several publications where similar RNAi-based methods are used in salmon louse, RNAi studies in salmon louse are challenging.

Sammendrag

Lakselus er en ektoparasittisk copepode på laksefisk. Den fører til betydelige økonomiske tap i oppdrettsindustrien, samtidig som den representerer en velferdstrussel for oppdrettslaksefisker og en mulig trussel mot ville anadrome laksefiskpopulasjoner. Eksperimentell posttranskripsjonell nedregulering av spesifikke gener ved RNA interferens (RNAi) er en metode for å karakterisere funksjonen til gener i mange organismer, inkludert lakselus, og eksperimentell RNAi har blitt oppnådd i flere av lakselusas utviklingsstadier. RNAi kan, sammen med andre teknikker, øke kunnskapen om interaksjoner mellom parasitt og vert, samt bidra til å identifisere molekylære mål for kjemisk behandling og mulige vaksineantigen.

I dette prosjektet ble de to genene *LsPale* og *LsTDO*, som koder for henholdsvis tyrosin hydroksylase (TH) og tryptofan 2,3-dioksygenase (TDO) hos lakselus, studert. De to enzymene er viktige i metabolismen av flere neurotransmittere, pigmenter og andre metabolitter av tyrosin og tryptofan. Fylogenetiske analyser viste at begge genene hører til sine artropode genfamilier, og at de er nært beslektet med tilsvarende gener i andre hoppekreps. En nedregulering av de to genene ved RNAi ble også forsøkt i lakselusas nauplii-larver. *LsPale* ble nedregulert suksessfullt, og nedreguleringen var detekterbart i mindre enn syv dager. Ingen morfologiske eller adferdsmessige endringer ble observerte tre og syv dager etter behandling, men larvene var inaktive rett etter at dobbeltrådet RNA (dsRNA) ble introdusert. Genuttryksprofiler av de to genene viste at *LsPale* er sterkt oppregulert før og gjennom den metamorfologiske forvandlingen til copepoditt og at *LsTDO* er uttrykt i både i lakselusas planktoniske og parasittiske utviklingsstadier, med en topp i preadult og adult.

Siden resultatene indikerer at genene er involvert i flere av lakselusas utviklingsstadier, burde det gjøres mer arbeid for å karakterisere de to genene. Videre medvirker sannsynligvis *LsTDO* i øyepigmentering, og kan potensielt fungere som en seleksjonsmarkør om CRISPR/Cas9-basert genredigering skal utvikles for lakselus. Dette prosjektet illustrerer også at RNAi i lakselus er utfordrende, til tross for flere publikasjoner der lignende RNAi-basert metodikk er benyttet.

Preface

The majority of work presented in this thesis was conducted at the Cell, Molecular Biology, and Genomics group (CMBG) and with the Taskforce Salmon Louse (TFSL) at the Norwegian University of Science and Technology's (NTNU, Trondheim, Norway) Department of Biology (IBI). All handling of and experiments with live salmon louse, were conducted at the NTNU SeaLab, and all molecular preparations and analysis, were performed at the CMBG labs.

I wish to thank my supervisor Atle Bones, head of CMBG, for giving me the opportunity to work on this project. A special thanks and a lot of gratitude is also needed for my co-supervisor Prashanna Guragain. He has given me excellent tutoring in the laboratory, valuable guidance when writing and answered all my questions. He has also given me the opportunity to work independently, which I have valued. A special thanks also goes to Torfinn Sparstad, for assistance with RNA isolation and qPCR analysis, and for always finding time to answer questions, and to Per Winge, which have assisted in assembling the genetic sequences and with phylogenetic analysis. A thank you is also needed for Anna S. Båtnes, Stine Østerhus and the rest of TFSL, as well as the rest of CMBG, for assistance and help, and for making me feel welcome and included.

Over the course of my five years as a biology student, I have had thousands of interactions with hundreds of people, both at NTNU and at the University of Agder. A very special thanks goes to all my peers in this period, for all the memories related to reading sessions, coffee breaks, excursions, and other events. Finally, I would like to thank my girlfriend and family, who have supported me over the course of my education.

A handwritten signature in cursive script, reading "Nanna Nikolai Opsahl". The signature is written in black ink on a light-colored background.

Trondheim, Norway

June 2021

Table of contents

Abstract	i
Sammendrag	iii
Preface.....	v
1 Introduction	14
1.1 The salmon louse	14
1.1.1 Background and life cycle	14
1.1.2 Pathogenicity	15
1.1.3 Consequences in salmonid farming.....	16
1.1.4 Implications for wild salmonids	16
1.2 RNA interference	17
1.2.1 History and biological relevance	17
1.2.2 Molecular mechanisms of experimental RNAi	17
1.2.3 RNAi in salmon louse	18
1.3 Tyrosine hydroxylase	20
1.4 Tryptophan 2,3-dioxygenase	22
1.5 Project aims	23
2 Methods.....	24
2.1 Gene identification and molecular characterization	24
2.2 Developmental expression profiling	25
2.2.1 Salmon louse maintenance.....	25
2.2.2 Collection of salmon louse developmental stages.....	25
2.2.3 Gene expression analysis	26
2.2.3.1 RNA isolation and cDNA synthesis	26
2.2.3.2 Relative gene expression measurements.....	27
2.2.3.3 Statistical analysis.....	27
2.3 Salmon louse RNAi	28
2.3.1 dsRNA production.....	28
2.3.1.1 Addition of T7 promoter by molecular cloning	28
2.3.1.2 Addition of T7 promoter by PCR	29
2.3.1.3 Synthesis of dsRNA	29
2.3.2 Salmon louse RNAi	29
2.3.2.1 Soaking of nauplii in dsRNA.....	29
2.3.2.2 Phenotype assessment	30
2.3.2.3 Gene expression analysis	30
2.3.2.4 Additional RNAi experiment	31

3	Results	32
3.1	Gene identification and molecular characterization	32
3.2	Developmental expression profiles.....	36
3.3	Gene expression and phenotypic traits following RNAi	38
3.3.1	Expression of genes in the catecholamine biosynthesis pathway.....	38
3.3.2	Phenotypic measurements.....	39
3.3.2.1	Swimming behavior and developmental pace.....	39
3.3.2.2	Body length and molting success	40
3.3.2.3	Cuticle Morphology	41
3.3.3	Results from additional RNAi experiment.....	42
3.3.4	Gene expression measurements from four discarded experiments	43
4	Discussion.....	44
4.1	A transient <i>LsPale</i> knockdown was likely achieved	44
4.2	<i>LsTDO</i> could be involved in the planctonic stages and the molt to copepodite ..	45
4.3	Expression profile suggests <i>LsTDO</i> contributes in adult maturation	46
4.4	Discarded experiments demonstrates the challenging of RNAi experiments in salmon louse.....	46
5	Conclusion	47
6	Future Work	48
	References	50
	Appendices	57

List of figures

Figure 1.1 The salmon louse developmental stages	15
Figure 1.2 Schematic illustration of RNA interference pathways	19
Figure 1.3 Overview of tyrosine metabolism	21
Figure 1.4 Overview of the kynurenine pathway in tryptophane metabolism	22
Figure 2.1 A salmon louse hatchery at the NTNU SeaLab	26
Figure 3.1 Predicted exon-intron structure of <i>LsPale</i> and <i>LsTDO</i>	32
Figure 3.2 Phylogenetic tree of tyrosine hydroxylase (A) and tryptophan 2,3-dioxygenase (B) proteins	33
Figure 3.3 Amino acid sequence alignment of salmon louse tyrosine hydroxylase.....	34
Figure 3.4 Amino acid sequence alignment of salmon louse tryptophan 2,3-dioxygenase.....	35
Figure 3.5 Developmental expression profiles of <i>LsPale</i> (A) and <i>LsTDO</i> (B)	37
Figure 3.6 Relative gene expression of genes in the catecholamine biosynthesis	38
Figure 3.7 Swimming behavior immediately after soaking	39
Figure 3.8 Body lengths and copepodite proportions.....	40
Figure 3.9 Cuticle morphology of stained copepodites	41
Figure 3.10 Swimming behavior (A) immediately after soaking, and cuticle imaging (B) and relative <i>LsPale</i> expression (C) three days after soaking	42
Figure 3.11 Results from RNAi experiments that were discarded	43

Abbreviations

ADT3	ADP/ATP carrier protein
Ago	Argonaute family protein
ANOVA	Analysis of variance
bp	Base pair
cDNA	Complementary DNA
Cop	Copepodite
DA	Dopamine
DDC	DOPA decarboxylase
DOH	Dopamine hydroxylase
dsCtrl	dsRNA complementary to an <i>Arabidopsis thaliana</i> LRK gene used as a mock control in RNAi experiments
dsPale	dsRNA complementary to <i>LsPale</i>
dsRNA	Double strand RNA
dsTDO	dsRNA complementary to <i>LsTDO</i>
<i>eEF1a</i>	Translation elongation factor 1a
gDNA	Genomic DNA
KF	Kynurenine formamidase
KMO	Kynurenine 3-monooxygenase
Kyn	Kynurenine
L-DOPA	L-3,4-dihydroxyphenylalanine
LB	Luria-Bertani
<i>LsPale</i>	Gene encoding tyrosine hydroxylase in salmon louse
<i>LsPAH</i>	Gene encoding phenylalanine hydroxylase in salmon louse
<i>LsTDO</i>	Gene encoding tryptophan 2,3-dioxygenase in salmon louse
miRNA	microRNA
mRNA	Messenger RNA
NADA	N-acetyldopamine
NBAD	N- β -alanyldopamine
NFK	N-formylkynurenine
NI	Nauplii I
NII	Nauplii II
nt	Nucleotide

PAH	Phenylalanine hydroxylase
<i>Pale</i>	Gene encoding tyrosine hydroxylase in <i>Drosophila melanogaster</i>
PCR	Polymerase chain reaction
PNMT	Phenylethanolamine-N-methyltransferase
qPCR	Quantitative real-time PCR
RISC	RNA-induced silencing complex
RITS	RNA-induced initiation of translational silencing
RNAi	RNA interference
rpm	Revolutions per minute
RXR	Retinoid X receptor
siRNA	Small interfering RNA
ssRNA	Single strand RNA
TH	Tyrosine hydroxylase
TS	Transcriptional silencing
W-o-L	Window-of-Linearity
WT	Wild type

1 Introduction

1.1 The salmon louse

1.1.1 Background and life cycle

The salmon louse (*Lepeophtheirus salmonis*, Krøyer, 1837) is a copepod of the Caligidae family. It is a marine salmonid ectoparasite on the northern hemisphere, that infests both wild and farmed salmonids. The salmon louse attack several economically and ecologically significant species, including Atlantic salmon (*Salmo salar*) and sea trout (*Salmo trutta*) (Dawson et al., 1997), arctic char (*Salvelinus alpinus*) (Bjørn et al., 2001) and rainbow trout (*Oncorhynchus mykiss*) (O'Donohoe et al., 2016).

The life cycle of the salmon louse consists of eight developmental stages, whereas three are planktonic and five are fully parasitic (Hamre et al., 2013) (Figure 1.1). Each developmental stage is separated by a molt. Nauplius I (NI) hatch from fertilized eggs, and have a 0.5 mm long and 0.2 mm wide semi-transparent body (Schram, 1993). The second nauplius stage (NII) is slightly larger, and precedes the infective copepodite stage (cop) (Hamre et al., 2013), which is around 0.6 mm long. The cop has a darker body color, and black and brown pigments beneath the cephalothorax on both sides of the intestine, around the eyes and on the trunk segments (Schram, 1993). The metamorphic transition of NII to cop involves significant changes in body plan and nervous system organization and complexity in copepods (Christie et al., 2014, Wilson and Hartline, 2011). Additionally, the crustacean eye often change significantly, as eyes of planktonic developmental stages are relatively basic compared to subsequent stages (Cronin and Jinks, 2001). The cop stage is followed by two parasitic chalimus stages, followed by two preadult and the sexually mature adult stage. (Hamre et al., 2013). Through the parasitic stages the salmon louse grows substantially, and the cephalothorax length of adult males and females are approximately 3 and 4.2 mm, respectively (Samsing et al., 2016). The salmon louse life cycle is direct, which means it only requires one host to complete it. Only the parasitic stages feed, as the pre-infective stages are lecithotrophic, meaning they depend on the energy reserves of the yolk sac (Eichner et al., 2015b).

The hatching time and length of the early larval stages are strongly correlated with water temperature (Samsing et al., 2016). At 10 °C, the naupliar larval stages lasts around 3.8 days and the infective window is more than 13 days long (Samsing et al., 2016).

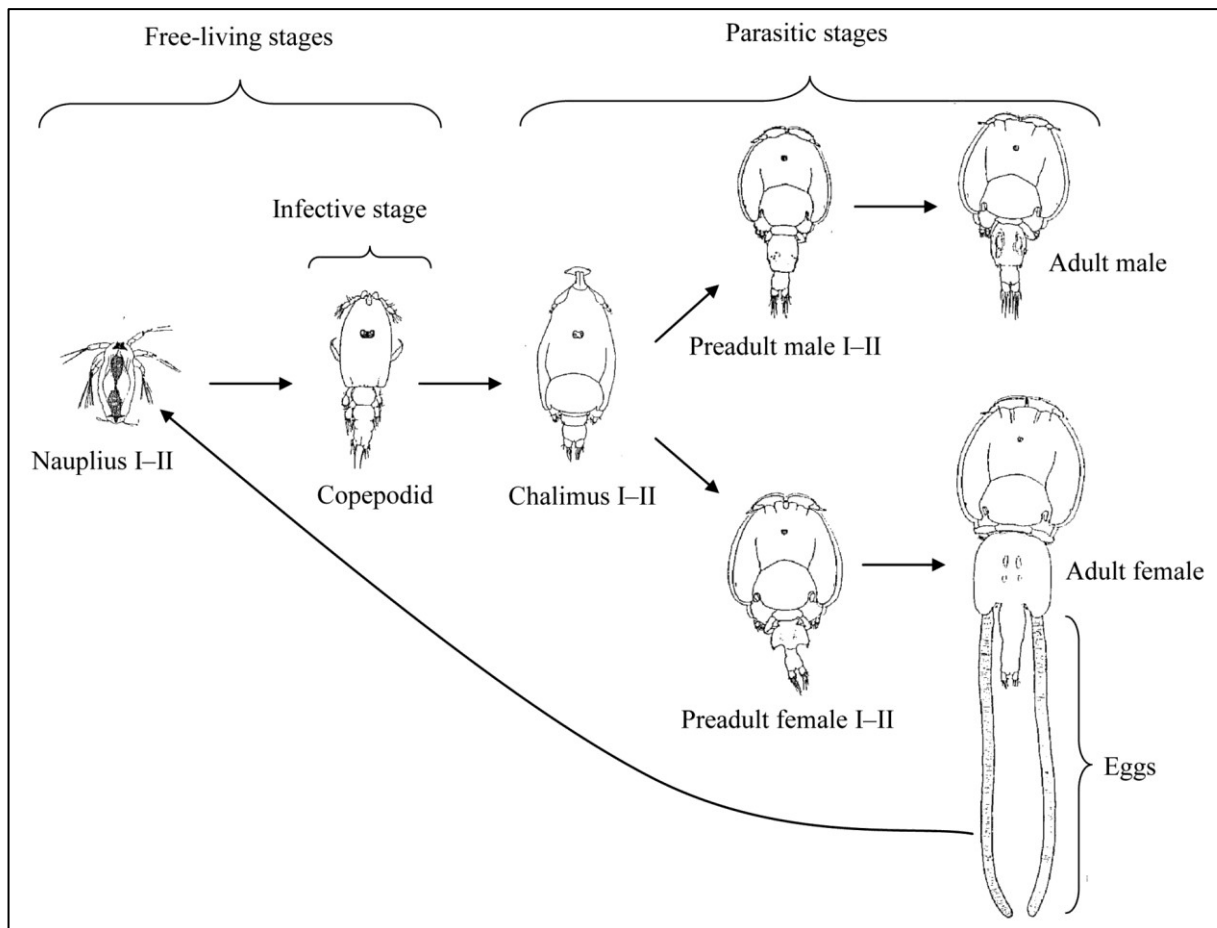


Figure 1.1 The salmon louse developmental stages

The two naupliar stages precede the infective copepodite stage. The transition from the free-living planktonic stages to the copepodite stage involve significant changes in body plan and neural system. The copepod then infects a host, where it develops through two chalimus stages and two preadult stages, before the sexually mature adult stage is reached. Female adults produce eggs, organized in strings that are attached to the abdomen. Nauplius larvae hatch from these eggs. The diagram is not to scale. Reprinted from Igboeli et al. (2014).

1.1.2 Pathogenicity

With rasping mouth parts, the salmon louse erodes and feeds on mucus, skin and underlying tissue to secure anchoring on and feed from the host (Costello, 2006). This results in epithelial degradation, osmotic stress, bleeding and increased mucus secretion with an altered biochemistry and microbiota (Costello, 2006, Llewellyn et al., 2017). Microbial defensive functions, including physical and chemical defenses, are compromised and the risk of secondary infections increases. Host salmonids show a reduced appetite and food-conversion, resulting in a reduced growth rate (Costello, 2006). Host leaping behavior also increases, which increases energy consumption and the risk of attracting predators (Costello, 2006).

Salmon louse infestations cause immunomodulation in hosts. In infested Atlantic salmon, certain immune-related genes are downregulated (Barker et al., 2019, Fast et al., 2006, Long et al., 2019). Further, peripheral blood monocytes collected from salmon louse infested Atlantic salmon have a reduced ability to reject salmonid alphavirus (SAV) infection, as well as an inability to upregulate several immune-related genes (Gamil et al., 2020). Salmon louse infestation also caused more severe secondary infections of the

infectious salmon anemia (ISA) (Barker et al., 2019) and infectious hematopoietic necrosis (IHN) (Long et al., 2019).

1.1.3 Consequences in salmonid farming.

Atlantic salmon in Norwegian fish farms have suffered from heavy salmon louse infestation since the industries' early days in the 1960s and 70s (Brandal and Egidius, 1977). The economic cost of parasite control have been steadily increasing through the following decades, and in 2006, the cost global cost of salmon louse control in aquaculture was estimated to be around €305 million (Costello, 2009). Estimates on the economic losses due to lost biomass growth caused by salmon louse infestation in Norwegian fish farms in 2011 range from 3% to 13% of total revenue (Abolofia et al., 2017). Since then, the total cost of preventive measures on Norwegian salmonid farms have quadrupled to 4 NOK per slaughtered kg salmon in 2018 (Iversen et al., 2019). The total yearly cost of these measures was estimated to 5 billion NOK per year in the Norwegian aquaculture industry (Iversen et al., 2019).

During the majority of the year, Norwegian law prohibits more than 0.5 mature female salmon louse per fish in Norwegian fish farms and this number is reduced to 0.2 during the warmest months (Forskrift om lakselusbekjempelse, 2012, §8). Salmon louse numbers are therefore continuously monitored, and strategies to reduce parasite burdens include medical and non-medical treatment (Iversen et al., 2019). Medical treatment is predictable and often effective, but extensive use has resulted in the development of salmon louse resistant to many of the substances used (Grefsrud et al., 2019), and spillover affect non-target crustaceans (Fairchild et al., 2010, Grefsrud et al., 2019, Parsons et al., 2020) and other organisms (Grefsrud et al., 2019, Tucca et al., 2014). Non-medical treatments include the use of lice skirts and lasers, as well as cleaner fish (Iversen et al., 2019). The general condition of the cleaner fish used in salmonid farms are a concern, and their mortality is high (Grefsrud et al., 2019).

1.1.4 Implications for wild salmonids

In the wild, juvenile salmonids suffer the most severe consequences from salmon louse infestation. Reduced swimming ability have been reported in pre-spawning Atlantic salmon and juvenile pink salmon (*Oncorhynchus gorbuscha*) when infested with adult salmon louse (Mages and Dill, 2010, Wagner et al., 2003), and in sockeye salmon (*O. nerka*), a high parasite load reduces foraging capacity (Godwin et al., 2015). Salmon louse thrives in environments with a high year-round host density, such as in areas with salmonid farms (Torrissen et al., 2013), and parasite numbers increase on wild salmonids if they coexist with farmed salmonids (Krkosek et al., 2005, Morton et al., 2004). In Ireland and Scotland, sea trout captured closer to salmon farms had higher salmon louse loads and reduced body conditions compared to trout captured further away (Shephard et al., 2016). A high salmon louse density in salmon farms located along Atlantic salmon migratory routes have a documented effect on post-smolt mortality: It increased 50 times in a Norwegian fjord during a high-density season compared to a low-density season (Bøhn et al., 2020). The mortality is also correlated with louse pressure in pacific salmon (Krkosek et al., 2011). Recently, salmon louse has been identified as one of the two main threats to several wild Atlantic salmon populations in Norway (Thorstad et al., 2020). These findings have contributed to the inclusion of wild Atlantic salmon on the tentative 2021 Norwegian Red List for Species (Norwegian Biodiversity Information Centre, 2021).

1.2 RNA interference

1.2.1 History and biological relevance

Almost three decades ago, it was discovered that transgene tobacco plants that expressed untranslatable sense and antisense transcripts of the coat protein gene of the tobacco etch virus (TEV), showed resistance to TEV infection (Lindbo and Dougherty, 1992). Some years later, Fire et al. (1998) demonstrated that, by introducing double stranded RNA (dsRNA) complementary to specific mRNA into the nematode *Caenorhabditis elegans*, post-transcriptional gene knockdown could be achieved. Since then, part of the role of small RNAs in gene regulation through RNA interference (RNAi) has been uncovered, and RNAi has emerged as a powerful and still expanding tool in reverse genetics (Wilson and Doudna, 2013).

RNAi is a highly conserved gene silencing mechanism in most eukaryotic organisms, that degrade target RNA transcripts in a sequence specific way (Cooper et al., 2018). The human genome encodes over 1000 microRNAs (miRNA), that contributes in the regulation of at least a third of human genes, including vital processes, such as cell growth, differentiation, and proliferation (Wilson and Doudna, 2013). RNAi mechanisms are also involved in eukaryotic defense against transposons (Cooper et al., 2018). In arthropods and several other invertebrates, RNAi mechanisms serve as the main antiviral defense (Schlee and Hartmann, 2016).

1.2.2 Molecular mechanisms of experimental RNAi

Experimental gene knockdown by RNAi utilizes a conserved enzymatic machinery (Cooper et al., 2018, Wilson and Doudna, 2013), and following the introduction of dsRNA, there are two main steps. Initially, the dsRNA is trimmed to smaller RNAs, known as small interfering RNA (siRNA) (Cooper et al., 2018). Then, the RNA-induced silencing complex (RISC) modifies and utilize the siRNA as a guide to knockdown the expression of specific genes, either through transcript degradation or translational silencing (Cooper et al., 2018) (Figure 1.2).

The initial trimming-step is performed by a protein complex that includes the RNase III endoribonuclease Dicer (Ciechanowska et al., 2021). The dsRNA is recognized and trimmed down to 19-21 nucleotides (nt) long siRNA molecules, with a 2 base pair (bp) 3' overhang at each strand (Cooper et al., 2018). The siRNA is then loaded into RISC, that include argonaute (Ago) family proteins. The loading is performed by Dicer, with the help of dsRNA-binding proteins or by dsRNA-binding domains associated with Dicer (Cooper et al., 2018). Ago, the catalytically active component of the complex, recognizes the 3' and 5' of one of the strands of the dsRNA, before the other is eliminated (Wilson and Doudna, 2013).

After formation, RISC patrols the cytosol, and binds single stranded RNAs (ssRNA) complementary to the remaining siRNA guide strand (Cooper et al., 2018). The nt 2-6 of the siRNA is known as the seed sequence, and a complementation with the target transcript here is critical for the silencing efficiency of RISC (Wilson and Doudna, 2013). In cases of perfect or near perfect complementarity, cleavage of the transcript can occur if Ago have endonuclease domains. Alternatively, non-endonucleolytic translational repression can occur, both before and after initiation (Wilson and Doudna, 2013). Translational repression is often followed by RISC recruiting factors that deadenylate or relocate transcripts to processing (P) bodies, where proteins related to mRNA decay are

located (Luo et al., 2018), ultimately resulting in transcript degradation. (Wilson and Doudna, 2013). After degradation, RISC might be released to bind and degrade additional transcripts.

During RISC assembly, one of the two strands of the siRNA is selected as a guide strand, and the remaining strand is eliminated (Wilson and Doudna, 2013). The mechanism behind guide strand selection is somewhat unclear, but the strand with the thermodynamically least stable 5' terminal end is more likely to act as a guide RNA (Wilson and Doudna, 2013). In a study on the human HeLa cell line, where several dsRNA were introduced, both strands were always included in RISC (Lisowiec-Wąchnicka et al., 2019). The study also showed that the introduction of mismatches or modified nucleotides could create a more predictable guide strand selection, which can potentially limit unwanted off-target effects and increase the efficiency of target gene knockdown.

In the fission yeast *Schizosaccharomyces pombe*, along with several fungi and plants, dsRNA can induce transcriptional silencing (TS) (Bhattacharjee et al., 2019). This is done by the RNA-induced initiation of TS (RITS) complex, that consists of Ago and additional proteins, as well as a siRNA guide (Alberts, 2014) (Figure 1.2). RITS binds transcripts as they emerge from RNA polymerase II, and initiates silencing by methylating nearby histones (Alberts, 2014). Proteins that inhibit RNA polymerases, recruit chromatin modifiers, and aid the formation and maintenance of heterochromatin then utilizes the methylated histones as docking sites (Bhattacharjee et al., 2019). In *S. pombe*, large blocks of heterochromatin are present in the centromeres, telomeres and in several loci with ribosomal DNA and meiotic genes (Bhattacharjee et al., 2019). Whether similar mechanisms can repress transcription in metazoans is not known, but some studies suggest that it may have been conserved to humans (Bhattacharjee et al., 2019).

1.2.3 RNAi in salmon louse

RNAi is a valuable tool for evaluating gene function in non-model organisms. In salmon louse, knockdown of target genes by RNAi have been achieved in various developmental stages and by different dsRNA delivery methods. Soaking NI in dsRNA through the molt to NII have resulted in a stable knockdowns detectable by real-time quantitative PCR (qPCR) from two to at least 12 days after soaking (Eichner et al., 2014). Microinjection of dsRNA into the haemocoel of preadults and adults have also been used (Dalvin et al., 2009, Tröbe et al., 2014).

Multiple studies have used RNAi to study the consequences of knocking down various genes in salmon louse. Genes with a suspected relevance in development and molting in *L. salmonis* have been targeted in NI. Phenylalanine hydroxylase (*LsPAH*) involved in tyrosine metabolism (Guragain et al., 2020) and several genes in the chitin synthesis pathway (Braden et al., 2020, Eichner et al., 2015c, Harðardóttir et al., 2019) have been knocked down, often leading to molting and swimming difficulties. A knockdown of the ecdysone receptor (*LsEcR*) in NI resulted in increased mortality and severe histological changes, and a tandem knockdown with the retinoid X receptor (*LsRXR*) resulted in molting arrest in NII larvae (Sandlund et al., 2016). Knockdown of the Na⁺/K⁺-ATPase in NI and preadult II resulted in abnormal neuronal activity, reproduction and muscle and intestinal development (Komisarczuk et al., 2018). In adult females, several genes with a suspected relevance to egg development have been knocked down. This has resulted in reduced or abolished egg string development (Tröbe et al., 2014), reduced number of offspring (Tröbe et al., 2015) or irregular offspring development (Dalvin et al., 2009,

Eichner et al., 2015a). These studies have all aided in the study of critical biological function and improved understanding of underlying biological mechanisms.

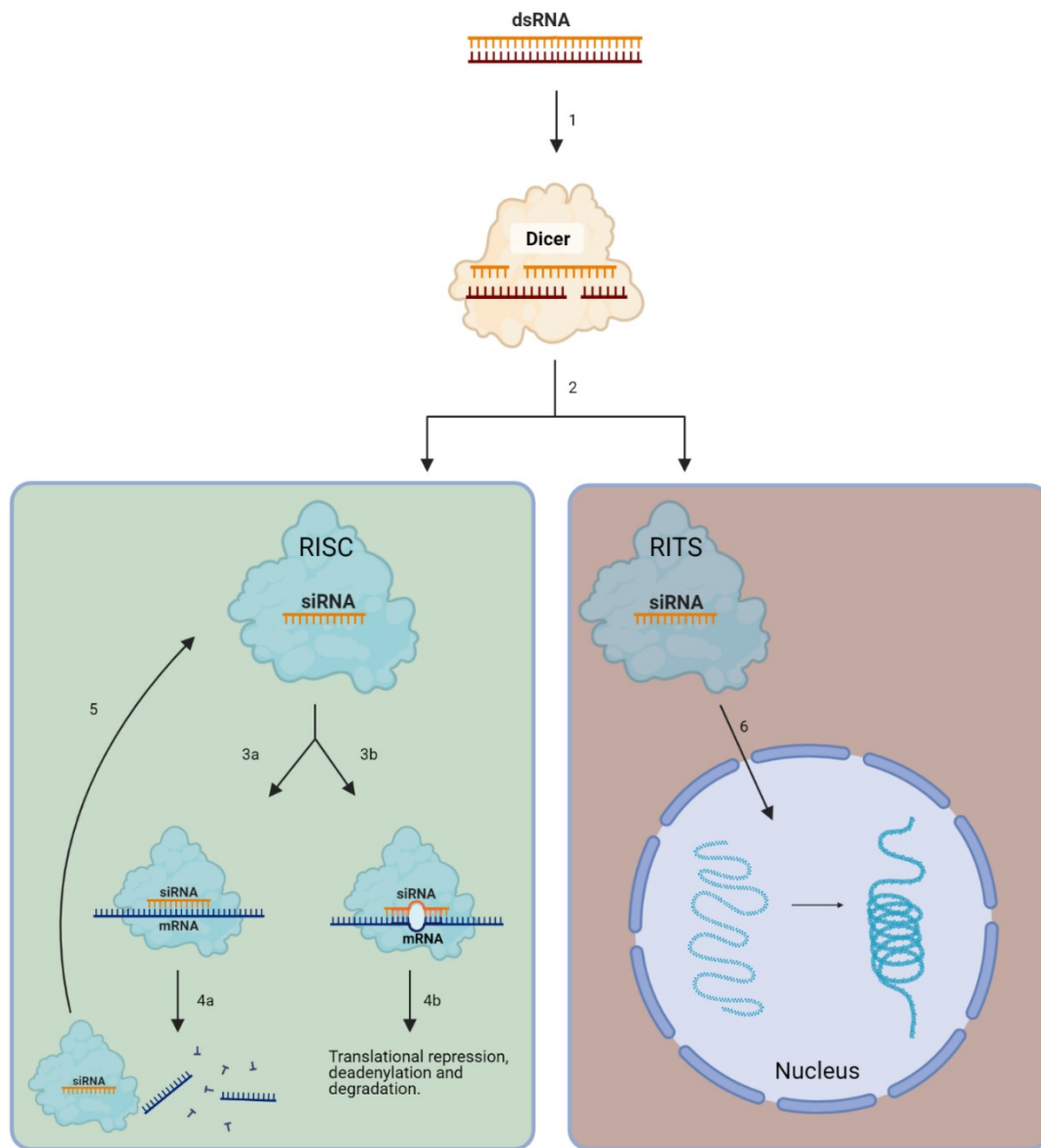


Figure 1.2 Schematic illustration of RNA interference pathways

Dicer process dsRNA into 19-21 nt long siRNA in the cytosol (1), before it is loaded into either the RNA inducing silencing complex (RISC) or the RNA inducing transcription silencing (RITS) complex (2). RISC binds mRNA and other transcripts with few or no mismatches to the guide siRNA (3a) or with more extensive mismatches (3b). If the complementarity between siRNA and transcript is perfect or near perfect, and RISC has endonuclease activity, the target transcript can be cleaved and degraded (4a). If the complementation is less extensive, translational repression before or after initiation, followed by deadenylation and degradation can occur (4b). If the transcript is degraded, RISC can be reused (5). RITS migrate to the cell nucleus (6), where it can bind to complementary transcripts as they emerge from RNA-polymerase II (not shown). From here, RITS can direct histone methylation, resulting in heterochromatin formation and selective transcriptional repression. This happens in the fission yeast *S. pombe*, and several plants and fungi. Whether RITS or similar mechanisms exists in metazoans, is unclear. Adapted from Cooper et al. (2018), Bhattacharjee et al. (2019) and "RNAi Mechanisms" (BioRender, 2021, retrieved from <https://app.biorender.com/biorender-templates>). Created with BioRender.com.

1.3 Tyrosine hydroxylase

Tyrosine hydroxylase (TH, EC 1.14.16.2) is a highly conserved tetrahydrobiopterin-requiring and iron-binding hydroxylase (Daubner et al., 2011). TH catalyzes hydroxylation of tyrosine to L-3,4-dihydroxyphenylalanine (L-DOPA) (Figure 1.3). L-DOPA is a precursor of the catecholamine neurotransmitters dopamine (DA), epinephrine and norepinephrine, as well as melanins and several metabolites important in sclerotization of the arthropod cuticle.

The biosynthesis of catecholamine neurotransmitters is important in the arthropod neural system. Loss-of-function mutations in the *pale* locus of *Drosophila melanogaster*, encoding TH, results in reduced DA levels and a shorter lifespan (Hanna et al., 2015). Further, N-acetyldopamine (NADA) and N- β -alanyldopamine (NBAD) (Figure 1.3) are secreted from the insect epidermis and incorporated in the cuticular matrix of insects during ecdysis (Andersen, 2010, Song et al., 2017). NADA has also been found in crustacean cuticle, indicating its involvement in crustacean sclerotization (Andersen, 2010). TH also plays a significant role in pigmentation of several arthropods. In *D. melanogaster*, a normal expression of TH and DOPA decarboxylase (DDC) are required for normal melanin patterning of the wings (True et al., 1999), and in the red flour beetle (*Tribolium castaneum*), TH knockdown reduces cuticle pigmentation (Gorman and Arakane, 2010). TH and DDC expression also match the pigmentation pattern of the Asian swallowtail (*Papilio xuthus*), where a normal pigmentation is prevented by inhibitors of these enzymes (Futahashi and Fujiwara, 2005).

The majority of knowledge of arthropod TH are from studies on insects. Less, however, are known about the enzyme's function in other classes of the phylum. In crustaceans, TH plays a role in physiological and behavioral development and function. It is found in the central nervous system of decapods (Laxmyr, 1985, Ponzoni, 2014, Ponzoni, 2017), and TH depletion increases pathogen resistance and alter the carbohydrate metabolism of whiteleg shrimp (*Litopenaeus vannamei*) (Mapanao et al., 2017). In the copepod *Calanus finmarchicus*, TH developmental expression pattern is similar to other enzymes involved in amine biosynthesis, including DDC and phenylalanine hydroxylase (PAH), with peaks in early nauplius and early cop (Christie et al., 2014). No work have been done on salmon louse TH, but Guragain et al. (2020) showed that *LsPAH* was expressed in a comparable manner in salmon louse as in *C. finmarchicus*, and that a knockdown of the gene did not modulate the expression of *LsPale* or any genes downstream in the catecholamine biosynthesis.

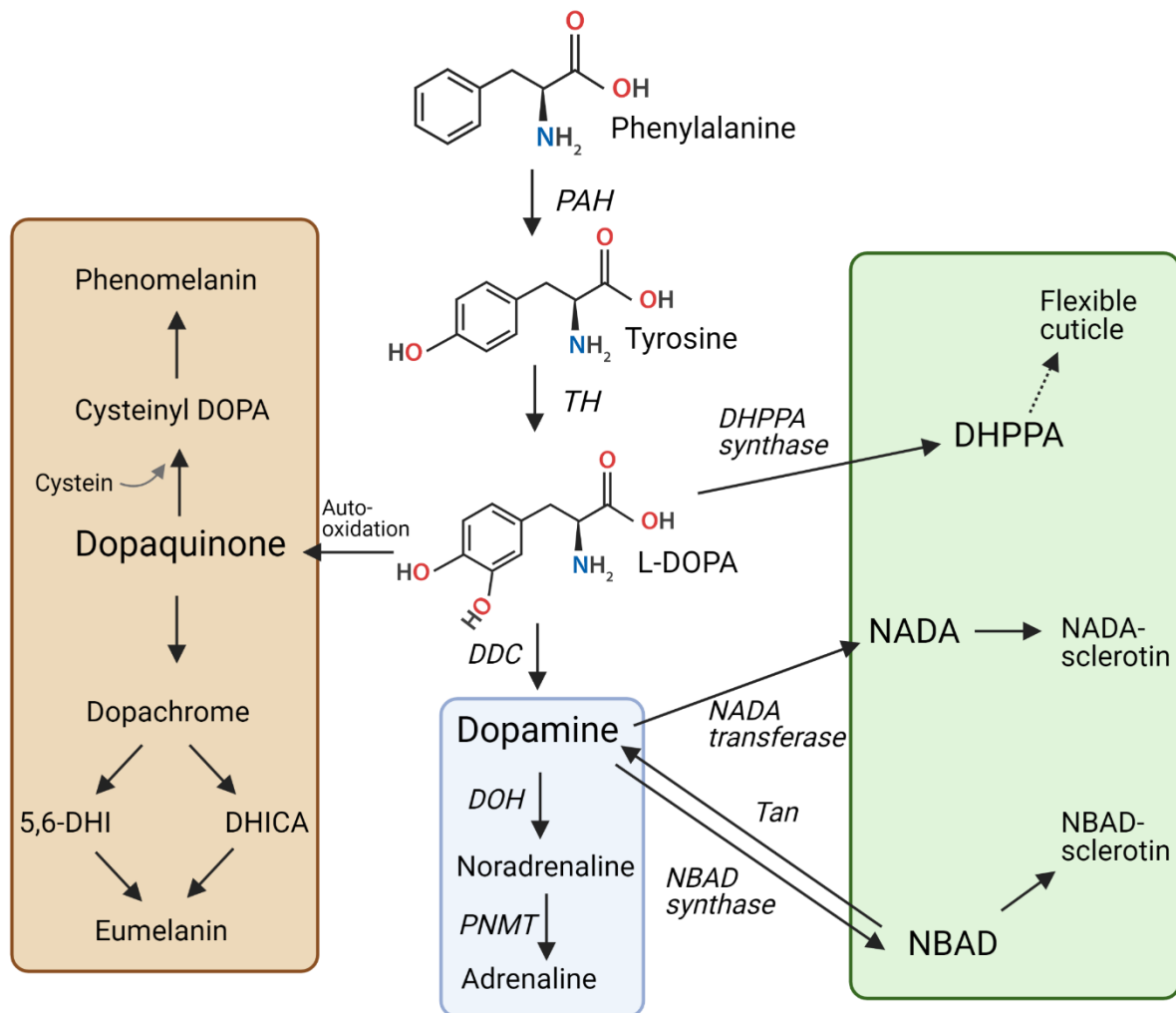


Figure 1.3 Overview of tyrosine metabolism

Tyrosine can be catalyzed from phenylalanine by PAH. TH then catalyzes the conversion of tyrosine to L-DOPA. L-DOPA is converted to several important metabolites, including melanins (highlighted in brown), catecholamines (highlighted in blue) and metabolites related to arthropod sclerotization and cuticle flexibility (highlighted in green).

Abbreviations: DDC – DOPA decarboxylase, DHICA – 5,6-dihydroxyindole-2-carboxylic acid, DHPPA – 3,4-dihydroxyphenylacetaldehyde, DOPA – L-3,4-dihydroxyphenylalanine, NADA – N-acetyldopamine, NBAD – N-β-alanyldopamine, PAH – phenylalanine hydroxylase, PNMT – phenylethanolamine-N-methyltransferase, Tan – NBAD hydrolase, TH – tyrosine hydroxylase and 5,6-DHI – 5,6-dihydroxyindole. Adapted from Guragain et al. (2020). Created with BioRender.com.

1.4 Tryptophan 2,3-dioxygenase

The essential amino acid tryptophan is the initial substrate in two key metabolic pathways: the tryptophan-serotonin pathway, where the neurotransmitter serotonin is synthesized, and the kynurenine (Kyn) pathway (Gostner et al., 2020). In the latter, tryptophan 2,3-dioxygenase (TDO, EC 1.13.11.11) catalyzes the conversion of tryptophan to N-formylkynurenine (NFK) (Figure 1.4) (Efimov et al., 2011, Zhang et al., 2007). Important products of the Kyn pathway include several neuroactive and immunoregulatory metabolites (Badawy, 2017).

In arthropods and cephalopods, a group of pigments known as ommochromes are also synthesized through the Kyn pathway (Figon and Casas, 2019). Skin pigmentation is reduced by knocking out the TDO gene in the squid *Doryteuthis pealeii*, and pigmentation is completely eliminated through an early knockout (Crawford et al., 2020). In arthropods, ommochromes are synthesized and located in ommochromosomes, membrane bound organelles in the ommatidia cells of the compound eye (Dontsov et al., 2020), where they play a role in photoprotection of the crustacean eye (Dontsov et al., 1999).

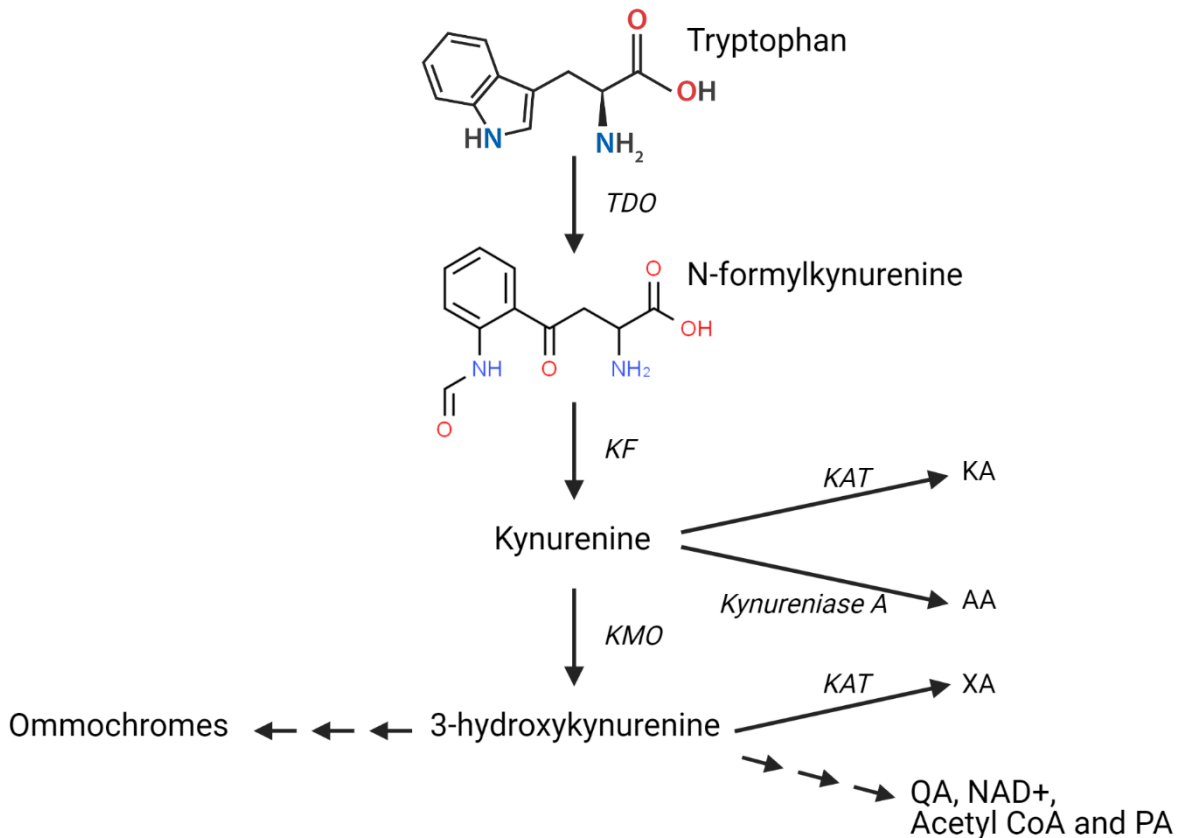


Figure 1.4 Overview of the kynurenine pathway in tryptophan metabolism

TDO catalyzes the conversion of tryptophan to N-formylkynurenine. Kynurenine and 3-hydroxykynurenine is then converted to several important active metabolites, including KA, AA, XA, QA, NAD⁺, Acetyl CoA and PA. In many invertebrates, including arthropods, 3-hydroxykynurenine is also converted to pigments known as ommochromes. Abbreviations: AA – anthranilic acid, KA – kynurenic acid, KAT – kynurenine aminotransferase, KFase – kynurenine formamidase, KMO – kynurenine 3- monooxygenase, NAD⁺ - nicotinamide adenine dinucleotide, PA – picolinic acid, QA – quinolinic acid, TDO – tryptophan 2,3-dioxygenase, XA – xanthurenic acid. Adapted from Badawy (2017) and Figon and Casas (2019). Created with BioRender.com.

1.5 Project aims

The aims of this project were to study expression and function of the two pigment-related genes *LsPale* and *LsTDO* in the salmon louse.

Research questions related to the project, were:

- I. What is the expression of *LsPale* and *LsTDO* in the various developmental stages of the salmon louse?
- II. Is there any evidence of developmental defects or other phenotypic changes in knockdown salmon louse larvae?

2 Methods

2.1 Gene identification and molecular characterization

The full-length complementary DNA (cDNA) sequence of all genes analyzed in this project, were assembled using salmon louse genome and transcriptomic data from NCBI Sequence Read Archive (SRA) database (Accession number SRX3788951). The intron-exon structures of *LsPale* and *LsTDO* were confirmed by aligning the cDNA sequence with the salmon louse genome sequences EMLSAG00000001561 and EMLSAG00000000516, respectively, in the Ensembl Metazoa genome browser (Release 51, EMBL-EBI; Howe et al., 2020). The two cDNA sequences are included in Appendix 1.

Phylogenetic analyses were done with amino acid sequences using MEGA7: Molecular Evolutionary Genetics Analysis version 7.0 (Kumar et al., 2016). The neighboring-joining algorithm were applied to matrices of pairwise distance estimates before the topology with the greater log-likelihood were chosen. To model the evolutionary rate differences among sites, a discrete gamma distribution was used [4 categories, (+G, parameter=1.1380)]. The trees were drawn to scale, with branch lengths measured in the number of substitutions per site. The *LsPale* sequence was compared to 12 other TH sequences, including three arthropodal. The *LsTDO* sequence was compared to 10 other TDO sequences, including three arthropodal sequences. The TH and TDO sequences were also aligned in the multiple sequence alignment tool GeneDoc v2.7 (Nicholas and Nicholas, 1997), and conserved amino acids and domains were identified. Accession numbers for all amino acid sequences used for phylogenetic analysis and alignment are listed in Appendix 2.

2.2 Developmental expression profiling

2.2.1 Salmon louse maintenance

All experiments and handling of fish in this project were conducted according to Norwegian regulations on animal research and welfare. Atlantic salmon (approx. 200 grams) were kept as host fish in 400 L tanks with a water flow of filtered seawater (250-450 L/h) in a climate-controlled room with a stable temperature of 10 °C. Temperature, salinity, water oxygen levels, general fish health and welfare, and parasite pressure and developmental progression were monitored daily.

The laboratory salmon louse strain *Ls Gulen* (Hamre et al., 2009) was kept at NTNU SeaLab on Atlantic salmon hosts. The strain was maintained by picking salmon louse egg strings from anesthetized fish. The host fish were then either returned to the tanks or euthanized, depending on factors such as the general health of the individual fish, the time as host and fish size. After picking, single egg strings were placed in tubes in a salmon louse hatchery (SLH) (Figure 2.1) and monitored daily. When salmon louse reached copepodite stage, the host fish were re-infested by turning off the water flow of the fish tanks and reducing the water level of the tanks to one third of the original level, before evenly spreading copepodites in the tank. After 30 minutes, the water flow was turned back to normal.

2.2.2 Collection of salmon louse developmental stages

Four biological replicates were prepared for each developmental stage. Each biological replicate contained either 50 NI, NII or cop, five chalimus I or II or one individual each of male or female preadult I, II or adult. The salmon louse were collected in 1.5 mL microcentrifuge tubes with lids, before water was removed and the samples flash frozen in liquid nitrogen. The samples were stored at -80 °C.

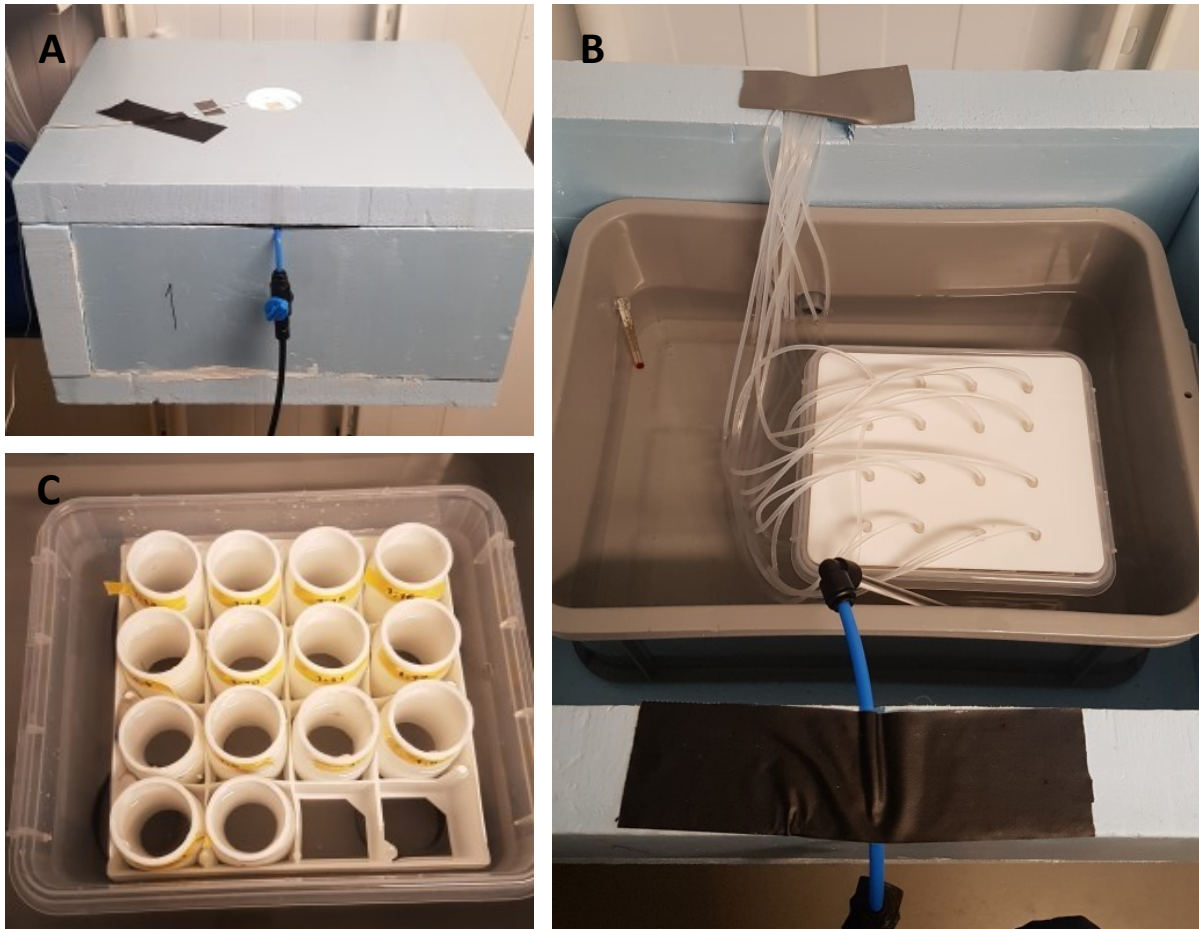


Figure 2.1 A salmon louse hatchery at the NTNU SeaLab

A – A salmon louse hatchery (SLH) made of a Styrofoam box with a lid and inside lighting through the lid.

B - Inside an SLH, a plastic tray was placed. Filtered seawater (10 °C) was flowing through the tray from the blue tube and was drained through a hole about 10 cm up the trays back wall. A plastic box with a lid with 16 holes was placed in the tray. A peristaltic pump (not shown) controlled a flow of 3 mL per minute filtered seawater (10 °C) through each hole in the plastic box lid. A thermometer was attached to the tray wall to monitor the water temperature.

C – A rack was placed inside the plastic box. It could support up to 16 PVC flow-through tubes (10 cm long), that were sealed off at the bottom end with 60 µm mesh. Pipette tips placed through the lid holes directed the water flow into each tube. A 2 cm gap between the tube bottom and the box bottom allowed the water to flow through the tubes. Excess water was drained from the plastic box through a hole halfway up the box's wall (not shown).

2.2.3 Gene expression analysis

2.2.3.1 RNA isolation and cDNA synthesis

The RNeasy mini kit (Qiagen) was used for total RNA extraction. The samples were transferred directly from storage at -80 °C into a TissueLyser II (Qiagen) adapter set and one 5 mm steel bead (Qiagen) were placed in each sample tube. Both the adapter set and the metal beads were cooled to -80 °C before use. The tissue was homogenized in a TissueLyser II at 25.0 Hz for 2.5 minutes. Quickly after homogenization, 600 µL of the Buffer RLT Plus lysis buffer with 2-mercaptoethanol was added to each sample. The homogenization was then repeated, before the mixture was centrifuged for 3 minutes at maximum speed. Genomic DNA (gDNA)-elimination and RNA washing were performed according to the RNeasy mini kit manufacturer's instructions. To maximize the yield, RNA

was eluted twice, using the primary eluate for the second elution. The RNA concentration and purity of the eluate was determined with a NanoDrop™ One/One® Microvolume spectrophotometer (Thermo Fisher Scientific). Purity was determined according to the absorption ratios described by Desjardins and Conklin (2010).

The QuantiTect Reverse Transcription kit (Qiagen) was used for gDNA wipeout and cDNA synthesis from the purified total RNA. This was done according to the manufacturer's instructions. cDNA was stored at -20 °C.

2.2.3.2 Relative gene expression measurements

Relative gene expression of target genes was measured by quantitative real-time PCR (qPCR) in a Roche LightCycler® 96 system. The salmon louse translation elongation factor 1a (*eEF1a*) (Frost and Nilsen, 2003) and ADP/ATP carrier protein (*ADT3*) (Eichner et al., 2015d) were used as reference genes. qPCR reactions were prepared according to Appendix 3, and primer pairs used for amplification of *LsPale* and *LsTDO* are listed in Appendix 4. All plates also included two non-template controls (NTC) per primer pair. NTCs were prepared by replacing DNA-template with PCR-grade water.

2.2.3.3 Statistical analysis

LinRegPCR v2015.4 (Academic Medical Centre, Amsterdam, the Netherlands) was used to calculate the average PCR efficiency for all primer pairs in the analysis. This was done by grouping fluorescence intensity data according to primer pair before the software estimated the baseline fluorescence and used it for a baseline correction. A Window-of-Linearity (W-o-L) was identified in log-transformed fluorescence curves, to determine the cycles of exponential increase in fluorescence. From the W-o-L, the PCR efficiency for each primer pair was calculated through linear regression.

qBase+ software v3.2 (Biogazelle, Zwijnaarde, Belgium) was used to normalize the input template cDNA in the PCR-reaction according to the reference genes and calculate the relative gene expression according to Hellemans et al. (2007). Input for the calculation included average PCR-efficiency for each amplicon group and C_t -values, together with sample name. A pairing of samples from the same developmental stage was used, and a one-way analysis of variance (one-way ANOVA) was performed with a significance level at 0.05. The Tukey-Kramer post-test was then used to compare all possibly pairings of developmental stages. qBase+ produced a table of pairwise comparisons of all developmental stages and a relative expression of the target gene scaled against the expression in NI.

2.3 Salmon louse RNAi

2.3.1 dsRNA production

2.3.1.1 Addition of T7 promoter by molecular cloning

Molecular cloning

PCR was prepared with *Ls* Gulen cDNA as template and *DreamTaq*-polymerase was used for elongation, according to Appendix 5. The primer pair *LsPale_Fw* and *LsPale_Rw* (Appendix 4) was used to amplify a 485 bp region of the *LsPale* gene. The product was examined in an 1% agarose gel according to Appendix 6 and purified with the Wizard® SV Gel and PCR cleanup kit (Promega), following the manufacturer's instructions. DNA concentration and purity were determined by NanoDrop.

The T7 promoter was added to the amplicons using the TOPO™ TA Cloning™ Kit for Sequencing (Invitrogen, Thermo Fisher Scientific), following the manufacturer's instructions. Rubidium chloride (RbCl)-competent DH5α *Escherichia coli* was then transformed with the pCR™4-TOPO® TA cloning vector (Appendix 7), as 2 µL of the vector was added to 200 µL freshly thawed bacteria. After a 30-minute incubation on ice, the bacteria were heat shocked for 30 seconds in a 42 °C water bath, before they were immediately put on ice. 1 mL of Luria-Bertani (LB) media, prepared according to Appendix 8, was added, before the bacteria were incubated for 1 hour at 37 °C and 220 rpm in an Innova 44 incubation shaker (New Brunswick™ Scientific). Different volumes (25, 50 or 100 µL) of the culture were then plated on LB agar plates with ampicillin prepared according to Appendix 8 and spread with a sterilized cell spreader. The plates were incubated at 37 °C overnight.

Screening by colony PCR and sequencing

To determine the insert size in vectors of transformed bacteria, 20 µL PCR-reactions with M13 forward and reverse primers (Appendix 4) were prepared according to Appendix 5. Single colonies were picked from the plates with transformed *E. coli* with a sterile pipette tip. The tip was then carefully dipped into a prepared PCR-reaction before it was dropped into a 13 mL cell culture tubes containing 3 mL LB-ampicillin media (Appendix 8). The bacterial cultures were incubated overnight at 37 °C and at 220 rpm in an incubation shaker. The PCR reactions were run according to Appendix 5, but with an initial 10-minute 95 °C lysis step to release plasmid DNA. The size of the PCR product was determined by electrophoretic separation in an 1% agarose gel (Appendix 6).

Plasmids from cultures with insert of the correct size were isolated with the E.Z.N.A.® Plasmid Mini Kit (Omega Bio-Tek), following the manufacturer's instructions. The DNA concentration and purity of the extracted plasmids were then determined by NanoDrop. The plasmid concentration was adjusted to 150-250 ng/µL, and 400 ng of plasmid and 5 µL of M13 Forward primer (Appendix 4) was added to a 1.5 µL microcentrifuge tube and sent for sequencing (Eurofins GATC). Remaining plasmids were stored at -20 °C. Sequencing results were analyzed with the SnapGene (v5.2) software (from Insightful Sciences; available at snapgene.com), to identify complete inserts in both orientations with no polymorphisms.

Isolated pCR™4-TOPO® TA cloning vectors containing inserts of a gene encoding a leucine rich repeat protein kinase (LRK) from *Arabidopsis thaliana* with no sequence

similarities with the *L. salmonis* genome, was provided by Prashanna Guragain (IBI, NTNU). The template sequence is included in Appendix 9.

2.3.1.2 Addition of T7 promoter by PCR

A 472 bp region of the *LsTDO* gene was amplified from *Ls* Gulen cDNA using LsTDO_Fw and LsTDO_Rw (Appendix 4), ligated into pCRTM4-TOPO[®] TA cloning vector and transformed into DH5a *E. coli*, before the insert size and orientation were verified by colony PCR and sequencing as described in chapter 2.3.1.1.

As this amplicon was only found in one orientation in the vector, a PCR based approach was used to add the T7 promoter to the template in both orientations. The two primer pairs T7_LsTDO_Fw + LsTDO_Rw and LsTDO_Fw + T7_LsTDO_Rw (Appendix 4) were used, and PCR was performed according to Appendix 5. The amplicons were purified with the Wizard[®] SV Gel and PCR Clean-Up System (Promega) and the concentration and purity measured by NanoDrop. The amplicon size was then assessed by gel electrophoresis in a 1% agarose gel (Appendix 6).

2.3.1.3 Synthesis of dsRNA

Isolated plasmids with inserts in both forward and reverse orientation were used for synthesis of dsRNA complementary to *LsPale* (dsPale) and *A. thaliana* LRK (dsCtrl). With these vectors as templates, 20 µL PCR reactions were setup according to Appendix 5 with the primer pair M13 Forward and M13 Reverse. The PCR products were extracted with the Wizard[®] SV Gel and PCR Clean-Up System (Promega) and used as templates for dsRNA synthesis.

For synthesizing dsRNA complementary to *LsTDO* (dsTDO), the amplicons with T7 promoters prepared as described in chapter 2.3.1.2 were used.

dsRNA was synthesized and precipitated with the T7 RiboMAX[™] Express RNAi System (Promega), following the manufacturer's instructions. After mixing the reactions containing the forward and the reverse RNA strands, the reactions were incubated at 75 °C for 5 minutes, followed by a 1 °C/min-ramp down of the temperature to 5 °C. After precipitation, the dsRNA was further purified with the RNeasy mini kit (Qiagen), following the manufacturer's instructions. The concentration and purity were assessed by NanoDrop, and the RNA integrity assessed by gel electrophoresis in a 1% agarose gel according to Appendix 6.

2.3.2 Salmon louse RNAi

2.3.2.1 Soaking of nauplii in dsRNA

Egg strings of the *Ls* Gulen strain were picked and incubated as described in chapter 2.2.1 and monitored every 12 hours. To determine the exact hatching time, the egg strings were monitored every 4 hours after they assumed a dark-brown or black color.

After hatching, 12-hour old NI were used in RNAi experiments. In a single experiment, four biological replicates of 30 NI each were soaked in either dsPale or dsTDO. Control treatments included the soaking of four biological replicates in dsCtrl (mock control) and four replicates in filtered seawater (wild type control (WT)). All soaking was done in 1.5 mL microcentrifuge tubes with lids, as 100 µL filtered seawater with 40 ng dsRNA/µL was added to the tube. Each tube was stored in a rack for 17 hours in a climate-controlled room (10 °C), before the salmon louse were transferred to a flow-through tube

in an SLH (Figure 2.1). A total of four experiments targeting *LsPale* and one targeting *LsTDO* was conducted this way.

2.3.2.2 Phenotype assessment

Swimming behavior and developmental monitoring

Shortly before nauplii were transfer to an SLH, the treatment tubes were placed on a plane surface and left undisturbed for five minutes. The swimming behavior of all groups were then observed and photographed.

At one, three and five days after soaking, 10 salmon louse were randomly picked from each treatment. The developmental stage was determined under a Axio Zoom.v16 (ZEISS) microscope with a Plan-NEOFLUAR Z 1x/0.25 FWD 56 mm objective, before they were put back into their original flow-through tube.

Developmental success and body length

All salmon louse were assessed and photographed with a AxioCam 506 color (ZEISS)-camera under the Axio Zoom.v16-microscope seven days after soaking. Salmon louse were classified as alive if intestinal movement could be identified, and only alive individuals were used for downstream application. The developmental stage for all salmon louse were determined, and the proportion that had successfully molted to the cop stage was found for all treatment groups. Following the assessment, two salmon louse were removed from each biological replicate and stored at 4 °C in 10% formalin (w/v in PBS). The biological replicates were then put in 1.5 mL microcentrifuge tubes with lids, before water was removed and the samples flash frozen in liquid nitrogen. The samples were stored at -80 °C.

Cop proportions for all treatment groups were compared using a Chi-squared proportion comparison. Body lengths were measured with ImageJ 1.53a (National Institute of Health, USA; Schneider et al., 2012) and compared in a one-way ANOVA. Both statistical comparisons were done in RStudio (RStudio team, 2020), and figures were made using the R-package ggplot2 (Wickham, 2016).

Cuticle morphology assesment

The salmon louse stored in 10% formalin were used to assess the cuticle morphology of the different larva from the different treatments. Their cuticle was stained in a Congo Red (Sigma Aldrich) solution (1.5 mg/ml H₂O) overnight, before they were placed in distilled water for 5 minutes and washed several times. ibiTreat 8-well chamber slide (ibidi GmbH) with a thin layer of 1% agarose were used as support, and the stained salmon louse were imaged using a photomultiplier tube (PMT) on a Leica DMI8 microscope (Leica) with a HC PL APO 10x/0.40 CS2 objective. A 561 nm laser line was used to excite the Congo red stain, and emission was detected in the range 597-711 nm.

2.3.2.3 Gene expression analysis

From the salmon louse stored at -80 °C, total RNA was isolated with the RNeasy mini kit (Qiagen) and cDNA synthesized with the QuantiTect Reverse Transcription kit (Qiagen), as described in chapter 2.2.3.1.

The relative expression of *LsPale*, *LsPAH*, *LsDDC*, *Ls Dopamine hydroxylase (DOH)* and *Ls Phenylethanolamine-N-methyltransferase (PNMT)* in dsPale treated salmon louse and

LsTDO in dsTDO treated salmon louse were measured by qPCR as described in chapter 2.2.3.2. Statistical analysis was done as described in chapter 2.2.3.3. The relative gene expression for all genes were grouped according to treatment and normalized against the WT expression.

2.3.2.4 Additional RNAi experiment

To investigate if a *LsPale* knockdown was detectable three days after dsPale treatment, two biological replicates with 30 NI each were soaked in dsPale and two biological replicates were treated as WT, as described in chapter 2.3.2.1. Following the 17-hour soaking period, swimming behavior were recorded as described in chapter 0. Each biological replicate was then moved to individual tubes in an SLH (Figure 2.1). Three days after treatment, the salmon louse were pictured under a microscope, flash frozen in liquid nitrogen and stored at -80 °C. Cuticle morphology was assessed as described in chapter 0 and the relative gene expression of *LsPale* was measured as described in chapter 2.3.2.3.

3 Results

3.1 Gene identification and molecular characterization

The cDNA sequences of *LsPale* and *LsTDO* (Appendix 1) were confirmed by amplification of cDNA using specific primers and sequencing of the T7 templates used for dsRNA synthesis.

Alignment of *LsPale* cDNA with the salmon louse genome suggested that it contains 12 coding exons (Location SuperContig [LSalAtl2s1080:515.319-519.772](#)) (Figure 3.1). The predicted open reading frame (ORF) encoded a 514 amino acid polypeptide with a predicted molecular mass of 58.9 kDa and isoelectric point of 5.4. The phylogenetic analysis suggested that *LsPale* belongs in the arthropod TH family, and closely related to another copepod TH gene (Figure 3.2A). Alignment of the *LsPale* (Figure 3.3) amino acid sequences against other TH sequences confirmed that the enzyme contained highly conserved domains.

LsTDO cDNA alignment suggested that the gene has one non-coding exon upstream of the ORF, and five coding exons (Location SuperContig [LSalAtl2s1080:35035-44729](#)) (Figure 3.1). The predicted TDO protein consists of 326 amino acids, has a molecular mass of 37.6 kDa and isoelectric point of 8.6. Phylogenetic analysis and amino acid alignment indicated that *LsTDO* belongs in the arthropod TDO family, and that several domains are conserved (Figure 3.2B and Figure 3.4).



Figure 3.1 Predicted exon-intron structure of *LsPale* and *LsTDO*

The *LsPale* and *LsTDO* transcripts were aligned with a salmon louse genome. Coding exons are shown as brown boxes, and non-coding exons are shown as green boxes with a brown lining. *LsPale* and *LsTDO* cDNA sequences are included in Appendix 1. Screenshot from the Ensembl Metazoa genome browser (Release 51, EMBL-EBI; Howe et al., 2020).

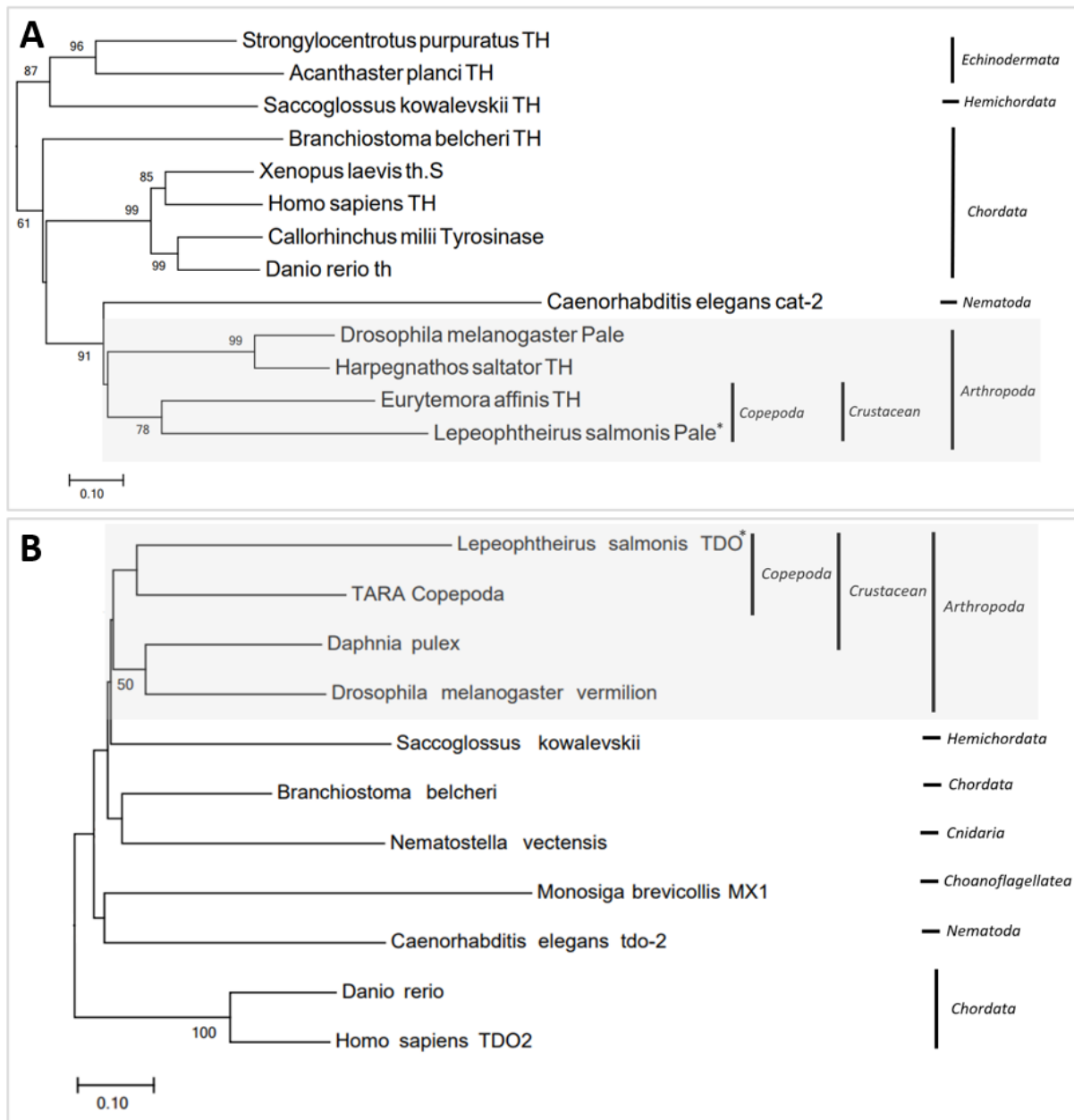
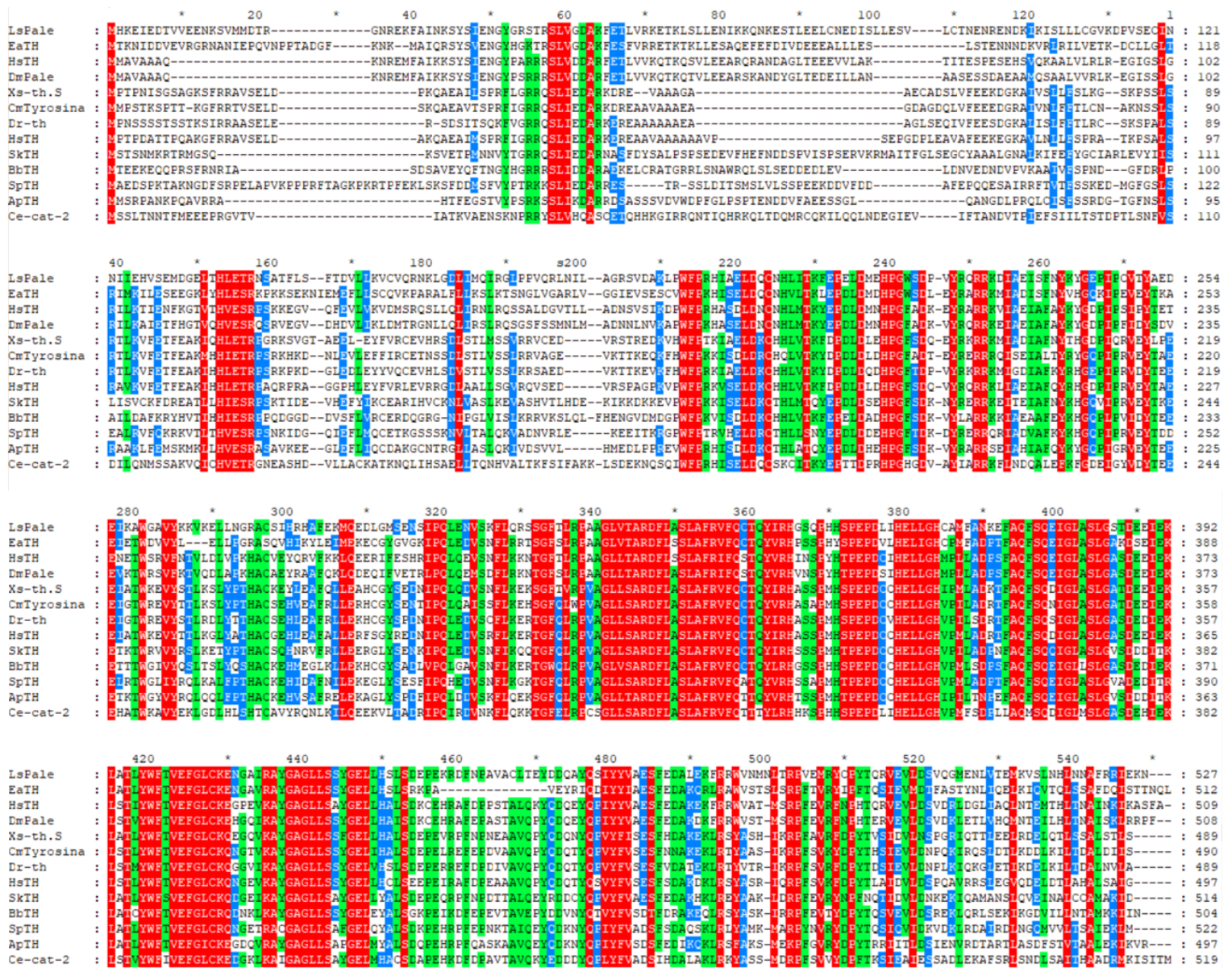


Figure 3.2 Phylogenetic tree of tyrosine hydroxylase (A) and tryptophan 2,3-dioxygenase (B) proteins

Bootstrap values are from 1000 replicates. Values below 50 are excluded. Branch lengths are number of substitutions per site. Arthropod protein families are highlighted with grey. The salmon louse genes are denoted with asterisks. Accession numbers for all amino acid sequences used are listed in Appendix 2. TARA Copepoda is derived from metagenomic copepod data from the TARA MATOU database (<https://tara-oceans.mio.osupytheas.fr/ocean-gene-atlas/>).



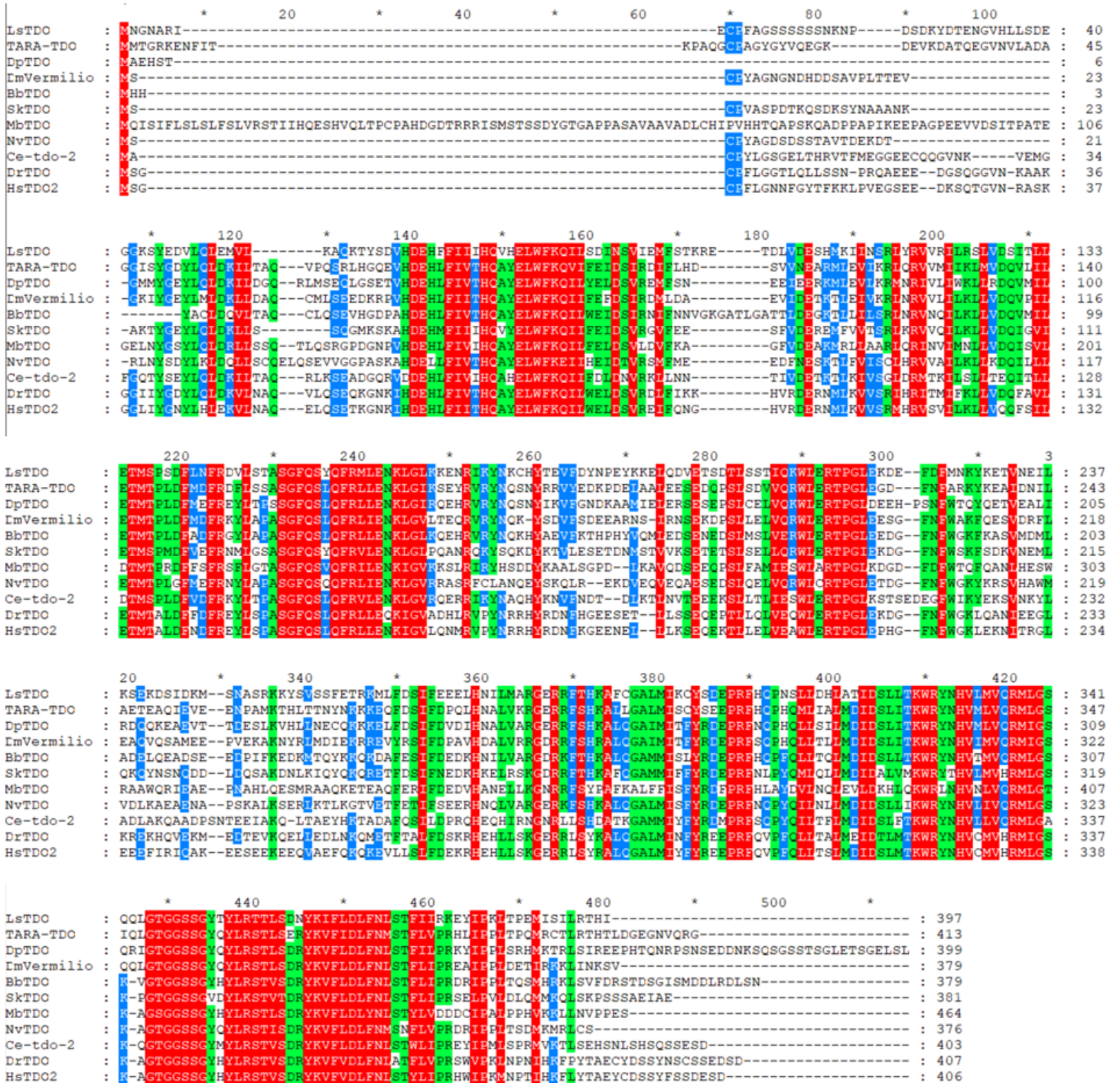


Figure 3.4 Amino acid sequence alignment of salmon louse tryptophan 2,3-dioxygenase

Salmon louse tryptophan 2,3-dioxygenase aligned with 10 TDO proteins. Colors highlight conserved sites (red = 100%, green = 80-100%, blue = 60-80%). Accession numbers for all amino acid sequences are provided in Appendix 2. TARA Copepoda is derived from metagenomic copepod data from the TARA MATOU database (<https://tara-oceans.mio.osupytheas.fr/ocean-gene-atlas/>).

Abbreviations:

- LsTDO - *Lepeophtheirus salmonis* TDO
- TARA-TDO - TARA Copepoda TDO
- DpTDO - *Daphnia pulex* TDO
- DmVermillion - *Drosophila melanogaster* vermilion
- BbTDO - *Branchiostoma belcheri* TDO
- SkTDO - *Saccoglossus kowalevskii* TDO
- MbTDO - *Monosiga brevicollis* TDO
- NvTDO - *Nematostella vectensis* TDO
- Ce-tdo-2 - *Caenorhabditis elegans* TDO
- DrTDO - *Danio rerio* TDO
- HsTDO - *Homo sapiens* TDO

3.2 Developmental expression profiles

The relative expression of *LsPale* and *LsTDO* were measured throughout all developmental stages from NI to adult by qPCR. The expression profiles indicates that both *LsPale* and *LsTDO* are expressed in all developmental stages (Figure 3.5). *LsPale* is highly expressed in the last two planktonic stages, as expression levels in NII and cop are significantly higher than in NI (Figure 3.5A). In the parasitic stages, *LsPale* expression levels are similar to NI, although the adult males have a significant increase in expression of *LsPale* compared to the other parasitic stages.

No significantly different expression of *LsTDO* was measured in the planktonic stages, although the highest expression levels were measured in cop (Figure 3.5B). Through the initial parasitic stages, including the first pre-adult stages, the expression was lower than in cop. Further, the expression profile indicate that *LsTDO* is gradually expressed at higher levels through the preadult stages, with the highest expression in adult males.

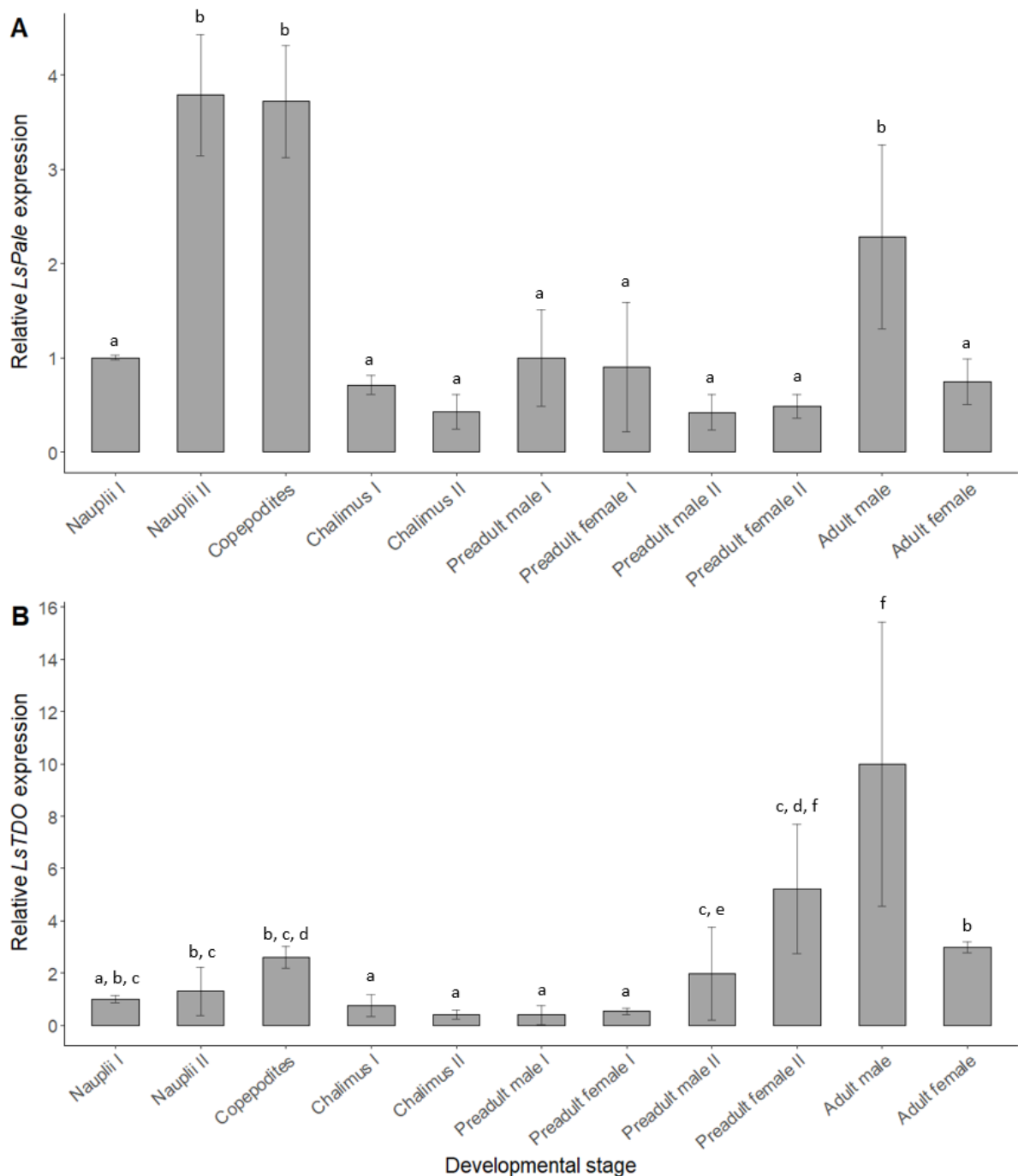


Figure 3.5 Developmental expression profiles of *LsPale* (A) and *LsTDO* (B)

Relative expression profiles for *LsPale* and *LsTDO* in the developmental stages of salmon louse. A one-way ANOVA with the Tukey-Kramer post-test was used to compare the relative gene expression measurements. Four biological replicates were prepared for each developmental stage. A single biological replicate consisted of either 50 nauplii I, nauplii II or copepodites, five male or five chalimus I or II, or one male or female preadult I or II or one adult. Error bars are standard error.

A - Nauplii II and copepodites showed a significantly higher expression of *LsPale* than nauplii I. Expression of *LsPale* in adult males were measured to be significantly higher than in the previous male developmental stages. Developmental stages labeled with different letters are significantly different from each other ($p < 0.001$).

B - No significant difference in *LsTDO* expression was measured in the planktonic stages, but the results indicate that it increases through the through the nauplius stages and into the copepodite stage. *LsTDO* expression increases significantly through the preadult stages for both sexes. The rise in expression continued into the adult stage for males. Developmental stages labeled with different letters are significantly different from each other ($p < 0.001$).

3.3 Gene expression and phenotypic traits following RNAi

3.3.1 Expression of genes in the catecholamine biosynthesis pathway

The analysis of the relative expression of genes in the catecholamine biosynthesis pathway were measured by qPCR seven days after soaking. The analysis indicated no significant knockdown of *LsPale* in dsPale treated salmon louse (Figure 3.6), but a marginally lower expression of the gene was measured. *LsPAH* expression was significantly higher in dsPale treated salmon louse compared to the controls, with a mean level of transcripts about three times as high as in WT. Of the genes downstream of *LsPale* in the catecholamine biosynthesis, no significant modulation of the expression was measured, but a slight increase in expression of *LsDDC* was observed.

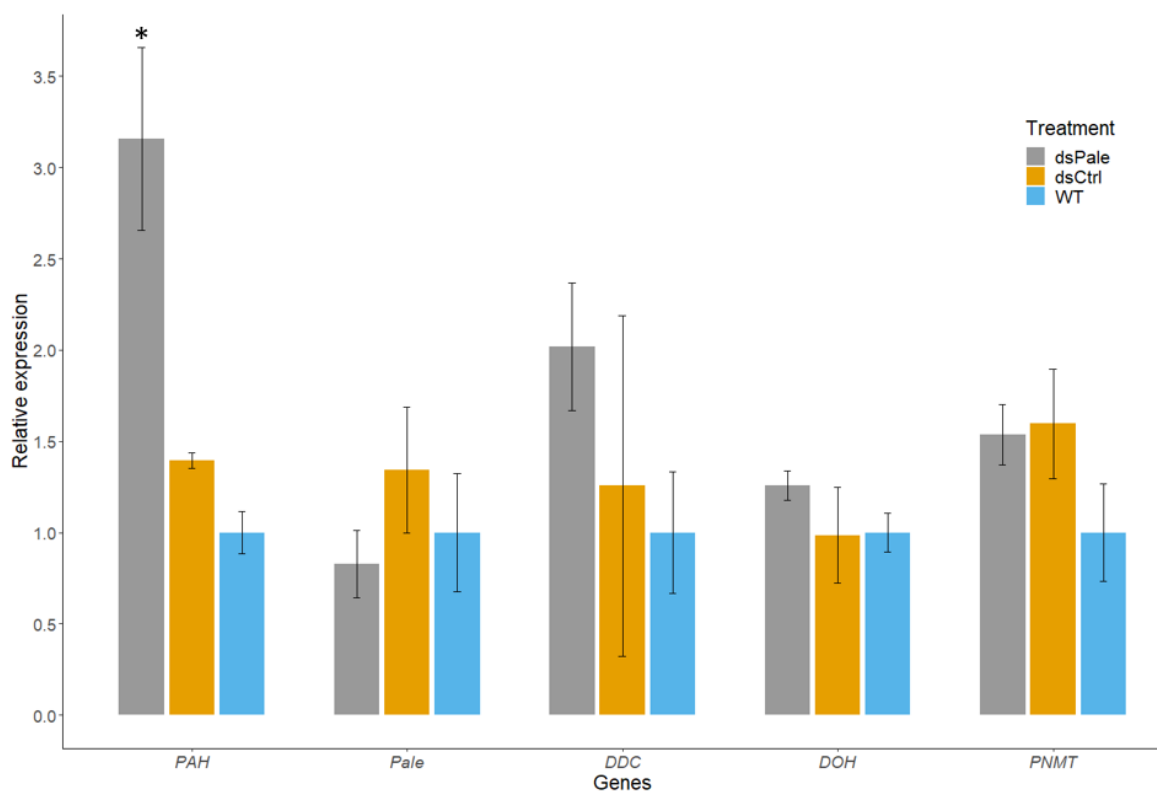


Figure 3.6 Relative gene expression of genes in the catecholamine biosynthesis

The relative gene expression levels of genes in the catecholamine biosynthesis measured seven days after soaking relative to WT. Only *LsPAH* was expressed significantly higher in dsPale treated salmon louse compared to the control treatments (mock control (dsCtrl) and WT). A marginally lower expression of *LsPale* and a marginally higher expression of *LsDDC* was also observed, but the differences were not significant compared to the control treatments. A one-way ANOVA with the Tukey-Kramer post-test was used to compare the relative gene expression measurements. The significantly different expression is denoted with an asterisk ($p < 0.0001$). Error bars are standard error.

3.3.2 Phenotypic measurements

3.3.2.1 Swimming behavior and developmental pace

Immediately following the dsRNA soaking, dsPale-treated NII appeared inactive compared to the controls and tended to cluster at the bottom of the treatment tube (Figure 3.7). However, a few anomalies were recorded, as the swimming activity of a few larvae was comparable to that of the dsCtrl and WT larvae.

At day one, three and five after treatment, observations of salmon louse from each treatment group suggested that WT larvae molted earlier than larvae treated with dsRNA. Copepodites were found in WT after three days, but none were found amongst the dsPale and dsCtrl-treated salmon louse before day five.



Figure 3.7 Swimming behavior immediately after soaking

Swimming behavior were assessed immediately after the soaking of nauplii in dsRNA to induce RNAi of *LsPale* (dsPale). Mock control (dsCtrl) and WT are control treatments. WT were soaked in filtered seawater. dsPale treated nauplii appeared more lethargic and accumulated at the bottom of the tube (red ring) compared to the control treatments, which were evenly distributed.

3.3.2.2 Body length and molting success

Seven days post treatment start, there was no difference in body length between dsPale treatment groups and the control treatments (Figure 3.8A). The mean body length in the three treatment groups were between 722 and 727 μm , and the majority of the salmon louse had a body length between 600 and 860 μm .

The proportion of salmon louse that successfully molted to cop was significantly higher in WT salmon louse compared to the two other treatment groups at day seven after soaking (Figure 3.8B). In WT, more than 80% of the salmon louse had successfully molted, compared to 45% and 52% in dsPale and dsCtrl, respectively.

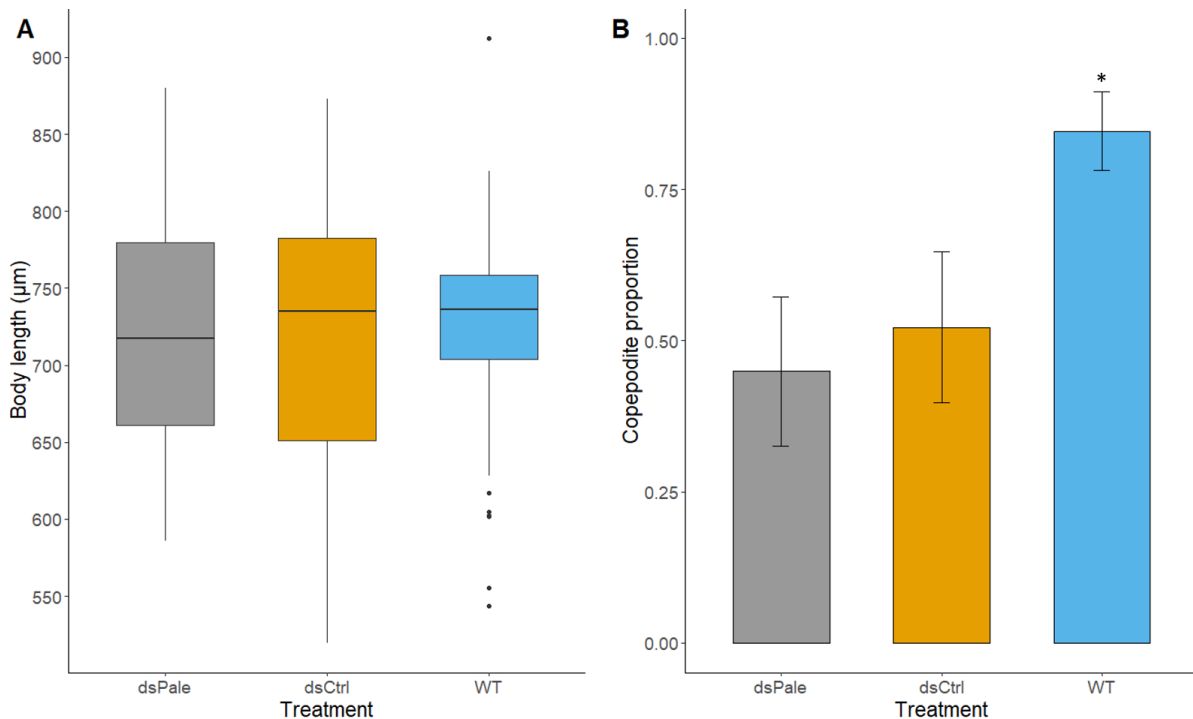


Figure 3.8 Body lengths and copepodite proportions

A – Body lengths seven days after soaking. Each box extends from the first to the third quartile, with the middle line indicating the median and whiskers stretching to the minimum and maximum lengths. Outliers were identified by the 1.5*IQR (inter quartile range)-rule. A one-way ANOVA indicated no significant difference in body length between the biological replicates ($p > 0.05$). B – Copepodite proportions seven days after soaking. The significantly different proportion is denoted with an asterisk ($p < 0.0001$). A chi-squared comparison of proportions was used to compare the three proportions. Error bars are standard error.

Mock control (dsCtrl) and WT are control treatments. $n=102-111$ for all treatments.

3.3.2.3 Cuticle Morphology

Imaging of Congo red stained salmon louse indicated no difference in cuticle morphology between the dsPale, mock control or WT treatments. dsPale treated larvae had the same body shape and abdominal segmentation as the controls (Figure 3.9), and no difference was observed in external appendages.

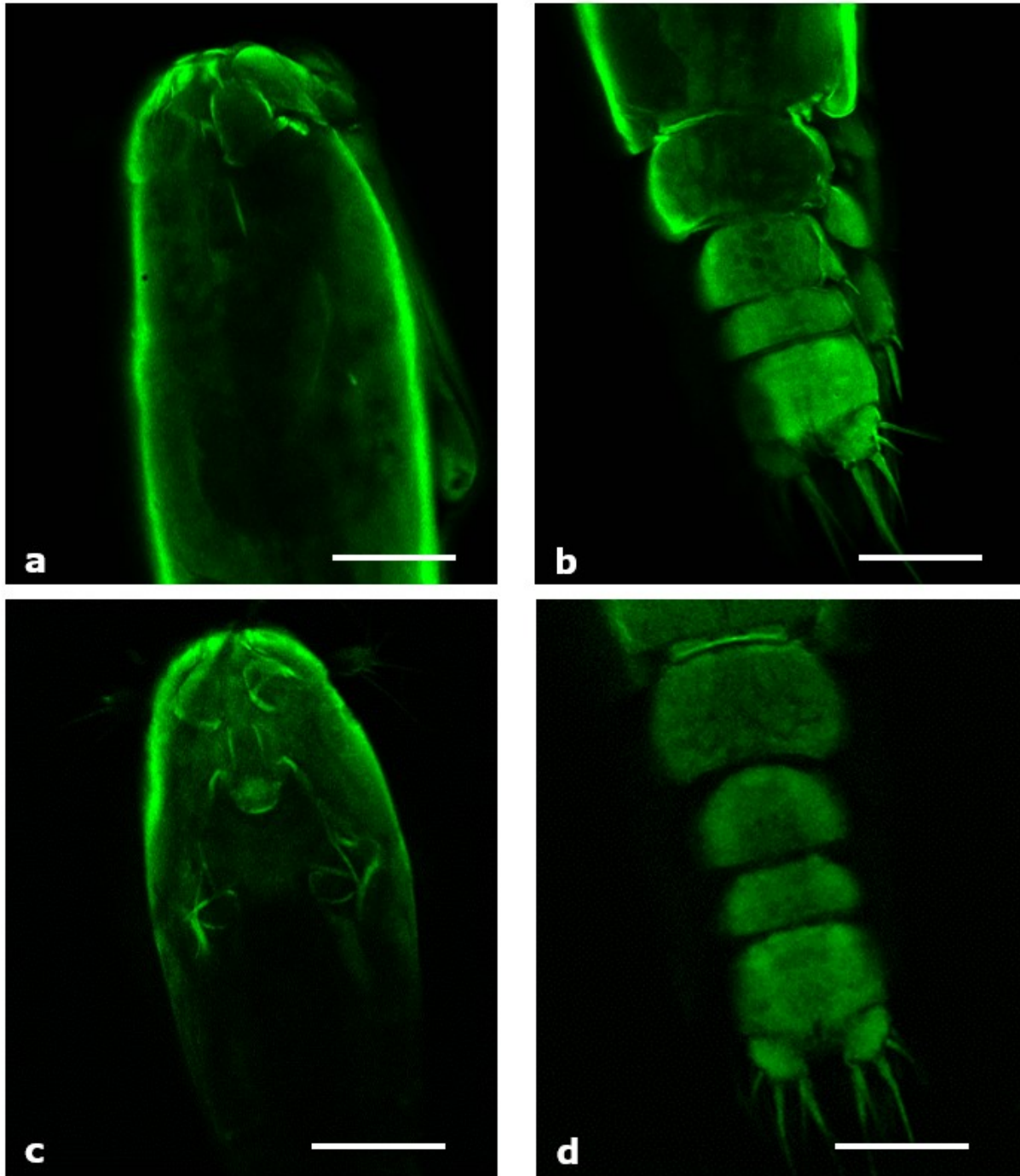


Figure 3.9 Cuticle morphology of stained copepodites

Cuticle morphology seven days after soaking. Upper panel: dsPale treated salmon louse. Lower panel: WT control. The cephalothorax (a, c) and abdomen (b, d) of a dsPale treated copepodite and a WT copepodite are depicted here. dsPale treated salmon louse showed no change in cuticle morphology. No difference in the shape of the cephalothorax or the abdominal segmentation were observed. Scale bars = 100 μ m.

3.3.3 Results from additional RNAi experiment

After soaking in dsPale, the salmon louse exhibited a similar swimming behavior to the one observed in the previously described experiment (chapter 3.3.2.1). dsPale treated salmon louse tended to accumulate at the treatment tube bottom, but some anomalies with a similar behavior to the controls were observed (Figure 3.10A).

When Congo red-stained salmon louse were imaged three days after soaking, all larvae were in the process of molting to cop, as ecdysis was observed (Figure 3.10B). Measurements of the relative *LsPale* expression in dsPale treated salmon louse showed a significantly lower gene expression compared to the expression in WT (Figure 3.10C). The mean expression level in the dsPale treatment was about one third of the expression in WT (p-value = 0.039).

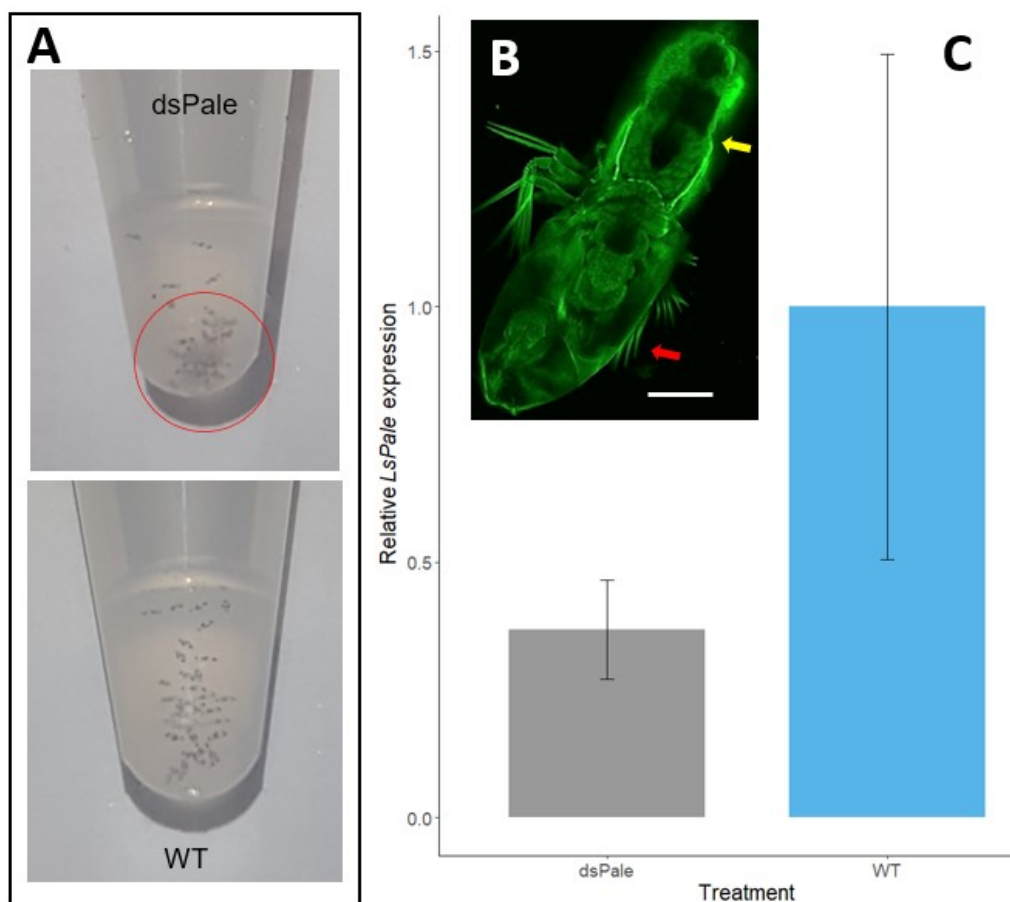


Figure 3.10 Swimming behavior (A) immediately after soaking, and cuticle imaging (B) and relative *LsPale* expression (C) three days after soaking

A – Swimming behavior were assessed immediately after soaking. WT is control treatment. dsPale treated salmon louse appeared more lethargic and accumulated at the bottom of the tube (red ring) compared to the WT, which were evenly distributed.

B – Salmon louse stained three days after soaking, were molting. A dsPale treated copepodite (yellow arrow) shedding its old cuticle (red arrow) is depicted here. Scale bar = 100 μ m.

C – The relative expression levels of *LsPale* were measured three days after soaking. An unpaired t-test showed that the *LsPale* expression in dsPale treated salmon louse was significantly lower compared to WT three days after soaking (p = 0.039). Error bars are standard error.

3.3.4 Gene expression measurements from four discarded experiments

A total of four RNAi experiments, one targeting *LsTDO* and three targeting *LsPale*, that were conducted in this project, yielded no usable results. In the experiment targeting *LsTDO*, a knockdown was not detected in dsTDO treated salmon louse and an extreme variation in expression of *LsTDO* was measured in the dsCtrl treatment groups (Figure 3.11A). As the salmon louse were observed under microscope seven days after treatment, it also became clear that the salmon louse was attacked by an infection, and that this had resulted in an extreme mortality rate (>50%) in all treatment groups.

Results from the additional three experiments targeting *LsPale* were also discarded. In one experiment, a significantly different expression of *LsPale* was measured in the two control treatments (mock control and WT) (Figure 3.11B). The remaining two experiments were run in parallel. No significant knockdown of *LsPale* was measured seven days after soaking (Figure 3.11C-D). In both experiments, the mortality rates were high (~50%). In one of these experiments (Figure 3.11C), an infection was identified the cause of the mortality, similar to the one observed in the experiment targeting *LsTDO*. In the other, the reason for the high mortality is unknown.

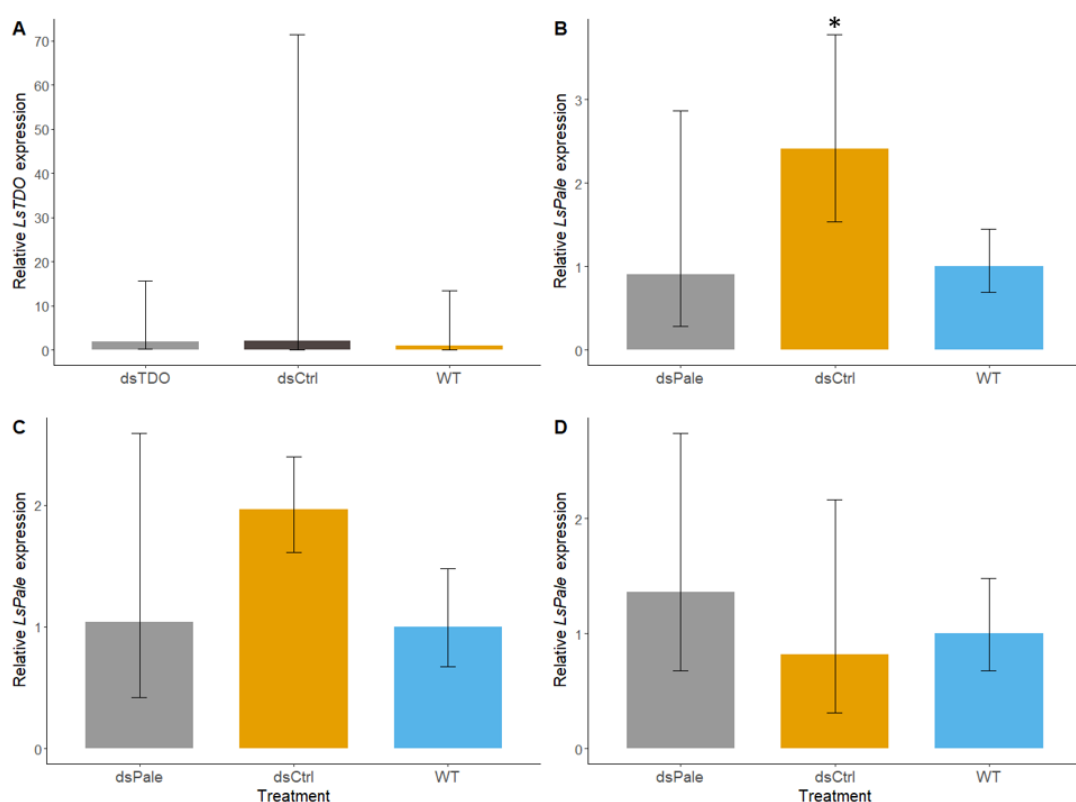


Figure 3.11 Results from RNAi experiments that were discarded

Gene expression measurements by qPCR seven days after soaking. A one-way ANOVA with the Tukey-Kramer post-test was used to compare the relative gene expression measurements. Gene expressions significantly different from WT are denoted with an asterisk ($p < 0.05$). Each treatment includes four biological replicates of (initially) 30 salmon louse each. Error bars are 95% confidence intervals.

A – *LsTDO* expression seven days after soaking of nauplii. The mock control (dsCtrl) had an extreme variation, and no significant difference were found between the treatments. Additionally, an infection yielded a high mortality rate (>50%) in all treatment groups. B, C and D – *LsPale* expression seven days after soaking of nauplii. Mock control (dsCtrl) was significantly different in B. No significant difference was found in C and D, but results were discarded due to a high mortality rate (~50%) in all treatment groups.

4 Discussion

4.1 A transient *LsPale* knockdown was likely achieved

TH catalyze the conversion of tyrosine to L-DOPA in the biosynthesis of catecholamine neurotransmitters (Daubner et al., 2011, Hanna et al., 2015), melanins (Futahashi and Fujiwara, 2005, True et al., 1999) and metabolites important in cuticle sclerotization in arthropods (Gorman and Arakane, 2010). Especially insect TH is well characterized, but the role of this enzyme in copepods and crustacean in general, is poorly understood.

Therefore, the aim of this project included identifying *LsPale*, that encodes TH in salmon louse, and study the expression of the gene and the function of salmon louse TH by inducing a RNAi-mediated knockdown in nauplius larvae. In the copepod *C. finmarchicus*, TH a distinct expression pattern in these developmental stages, as they are upregulation in early nauplius and copepodite (Christie et al., 2014). In the salmon louse, the expression of *LsPAH*, the gene upstream of *LsPale* in the metabolism of tyrosine, increases through the planktonic stages (Guragain et al., 2020). A RNAi-induced knockdown of *LsPAH* resulted in molting arrest, morphological defects and irregular body shape seven days after soaking in dsRNA (Guragain et al., 2020). The metamorphic transition from nauplii to cop involve significant changes in the organization of body plan and nervous system (Christie et al., 2014, Wilson and Hartline, 2011). This led to the formulation of the hypothesis that *LsPale* have a significant role in the NII-to-cop transition of salmon louse, and that a knockdown would compromise this process.

The gene was successfully identified, and the molecular characterization of the gene revealed that the gene is part of the arthropod TH gene family (Figure 3.2A) and that several domains of the enzyme are conserved (Figure 3.3), indicating a conserved catalytic function of the enzyme in eukaryotes.

The developmental expression profile of *LsPale* indicated a higher expression of the gene in NII and cop compared to NI (Figure 3.5A). This pattern is similar to the pattern of *LsPAH* expression in salmon louse (Guragain et al., 2020) and the expression of TH in *C. finmarchicus* (Christie et al., 2014). This suggests that *LsPale* is involved in the transition from NII to cop in salmon louse, possibly with a comparable role to *LsPAH* (Guragain et al., 2020). However, seven days after soaking in dsRNA, the gene expression measurements indicated no knockdown of *LsPale* (Figure 3.6), and no morphological or behavioral changes were observed. The method of dsRNA delivery by soaking NI through the molt to NII has previously resulted in substantial knockdown of several targeted genes from two to 12 days post soaking (Eichner et al., 2014). cDNA from *Ls Gulen* was used to make templates for dsRNA synthesis, and the templates were sequence to ensure full length complementation between dsRNA and the assembled transcripts. It was therefore expected that dsRNA soaking would induce a significant knockdown of *LsPale*. A reduced swimming activity was recorded in salmon louse immediately after being soaked in dsRNA complementary to *LsPale* (Figure 3.7), similar to the swimming behavior described by Guragain et al. (2020) in *LsPAH* knockdown salmon louse larvae. The expression of *LsPAH* was also significantly higher in dsPale treated salmon louse compared to control treatments seven days after soaking (Figure 3.6), and a minor, non-significant increase in transcripts was also measured of *LsDDC*.

These findings indicated a transient knockdown that either ended or was reduced to a non-detectable level seven days after introduction of dsRNA.

Therefore, a shorter, small-scale (due to capacity limitations) experiment was performed to further investigate this, where two biological replicates were treated with ds*Pale*, and two biological replicates underwent WT treatment. Three days after soaking, gene expression analysis of *LsPale* indicated a successful knockdown of the gene (Figure 3.10C), and salmon louse exhibited similar swimming behavior as recorded in the initial experiment (Figure 3.10A). These results strengthen the assumption that the knockdown of *LsPale* was transient or reduced at day seven. Further, these findings might indicate that *LsPale* is under the control of powerful negative feedback mechanisms to avoid potential damaging effects of low TH levels in the molt from nauplii to cop. Additionally, the significant upregulation of *LsPAH* seven days after soaking (Figure 3.6) could suggest that this gene is also controlled by connected feedback mechanisms when *LsPale* is knocked down. As *LsPAH* catalyzes conversion of phenylalanine to tyrosine, the step upstream of TH in tyrosine metabolism, this might be a response to depletion of tyrosine metabolites in the salmon louse.

No other phenotypic measurements or observations were performed on salmon louse larvae at three days after soaking, as they were molting at this time (Figure 3.10B). This is in accordance with Samsing et al. (2016), which reports that the molt to cop at 10 °C take place about 3.8 days after hatching. Molting would affect body length measurements, the observed body shape and other phenotypic traits that could possibly be used to characterize the phenotypic effect of a *LsPale* knockdown after three days.

Only two biological replicates per treatment were included in the three-day long follow-up experiment and observed p-value of 0.039 in the gene expression analysis was only marginally below the common threshold for significance (0.05). Thus, it cannot be completely concluded whether or not *LsPale* can be knocked down by the approach described in this thesis. Although the swimming behavior and modulation of *LsPAH* expression suggest a transient knockdown occurred between soaking and day seven, no knockdown was measured on day seven, and no phenotypic measurements or observations indicate that the transient knockdown influenced any phenotypic traits. Thus, no conclusions about the function of TH in salmon louse NII and cop can be drawn.

4.2 *LsTDO* could be involved in the planctonic stages and the molt to copepodite

The conversion of tryptophan to NFK is catalyzed by TDO. Through the Kyn pathway, NFK is converted to neuroactive and immunoregulatory metabolites (Badawy, 2017), as well as ommochromes in arthropods (Figon and Casas, 2019). Little work has been conducted on the function of TDO in copepods. An aim of this project was therefore to identify *LsTDO* and to study the expression of the gene and the function of salmon louse TDO by inducing a RNAi-mediated knockdown in nauplius larvae. Ommochromes are essential in photoprotection of the crustacean eye (Dontsov et al., 1999), and the crustacean eye is complexified through the transition from the nauplius larva to subsequent stages (Cronin and Jinks, 2001). Further, TDO knockout reduced pigmentation in the squid *D. pealeii*. From this, the hypothesis that a *LsTDO* was expressed in the planktonic stages of the salmon louse and that a knockdown would result in noticeable changes in the pigmentation of the cop eye was developed.

The phylogenetic analysis indicate that *LsTDO* is closely related to other arthropod TDO genes (Figure 3.2B), and amino acid alignment with other eukaryotic TDO sequences indicated that important protein domains are conserved (Figure 3.4), suggesting a that the enzyme's catalytic function is conserved.

The developmental expression profile of *LsTDO* suggests that the gene is expressed in all the developmental stages of the salmon louse. Furthermore, a slight, but not statistically significant, increase in expression through the planktonic stages was measured (Figure 3.5B). These results indicate that TDO plays a role in these stages, and it could suggest the enzymes involvement in the NII-to-cop transition. As the attempted knockdown of *LsTDO* by RNAi was not successful, the effect of *LsTDO* in the molt to cop remain unknown, and additional experiments attempting RNAi-induced *LsTDO* knockdown should be conducted to identify the function of the gene in planktonic developmental stages and in the transition to cop.

4.3 Expression profile suggests *LsTDO* contributes in adult maturation

The *LsTDO* expression increases significantly through the preadult stages in both sexes, and into the adult stage in males (Figure 3.5B). This indicates that the gene is involved in development through the latter parasitic stages of the salmon louse. As several neuroactive and immunoregulatory metabolites are synthesized through the Kyn pathway (Badawy, 2017), along with ommochromes (Figon and Casas, 2019), the role of the enzyme is unclear. The salmon louse's body size increases considerably through these stages (Samsing et al., 2016) and sexual maturity is reached in the adult stage. Consequentially, TDO could serve several functions through this maturation. The role of TDO in copepods are still poorly understood, and further work should be performed to better understand the function of this enzyme through the copepod life cycle.

4.4 Discarded experiments demonstrates the challenging of RNAi experiments in salmon louse

Four RNAi experiments, one targeting *LsTDO* and three targeting *LsPale*, were also conducted, but their results discarded. This was done due to high mortality rates caused by infections and other unknown reasons, along with high variation in the gene expression measurements and significantly different gene expression in control groups (Figure 3.11A-D). These difficulties illustrate the challenge of working with RNAi in salmon louse and other non-model organisms, where measures to reduce mortality, variation in measurements and so on are less known. By continue to work with and study the salmon louse, it should be possible to reduce these challenges, ensuring an increase in the pace of discovery in salmon louse, copepods, and crustaceans.

5 Conclusion

The aim of this project was to study the expression and function of the two pigment related genes *LsPale* and *LsTDO* in the salmon louse. This was done by measuring the developmental stage expression and inducing RNAi-mediated knockdown of the genes in early developmental stages, followed by identifying induced phenotypic changes and modulation in expression of genes in relevant metabolic pathways.

LsPale was expressed in all developmental stages of the salmon louse, and the expression increased before and through the metamorphic molt from NII to cop. A *LsPale* knockdown was achieved, but it was detectable for less than seven days. This could indicate that powerful negative feedback mechanisms control the expression of the gene, as well as other genes involved in the biosynthesis of catecholamine neurotransmitters. The only induced phenotypic change was a reduced swimming behavior immediately after soaking in dsRNA, and no other phenotypic changes were identified three and seven days after treatment.

No knockdown of *LsTDO* was achieved, but the expression profiles point to a role in the planktonic stages in the salmon louse, as well as in the maturation through the parasitic stages of both sexes. TDO catalyzes the initial step in the biosynthesis of neuroactive, immunoregulatory metabolites and ommochromes, but its role in the salmon louse is still unclear.

6 Future Work

In the future, the function of *LsPale* and *LsTDO* should be further studied in salmon louse. RNAi induced knockdown of *LsPale* appears to be transient, possibly due to the effect of strong feedback mechanisms. A method to create knockout lines should be applied to characterize the function of this and other genes. This could potentially be achieved by adapting CRISPR/Cas9 technology for salmon louse. dsRNA delivery by microinjection in preadult and adult salmon louse have already been used to successfully induce RNAi, and similar methods could possibly be used to deliver Cas9 nucleases and guide RNA (gRNA)-ribonucleoproteins or plasmids containing Cas9-gRNA gene cassettes.

When developing CRISPR/Cas9 technology, a suitable selection marker is necessary. The role of *LsTDO* in salmon louse is still unclear, but due to its likely involvement in eye pigmentation, this gene could be suitable. In the future, the function of *LsTDO* should be studied further, and additional attempts at knocking down the gene by RNAi should be conducted. Alternatively, microinjection to induce knockout of *LsTDO* by CRISPR/Cas9 technology could be done to explore the function of the gene and the potential of the genome editing technology in salmon louse simultaneously.

By expanding the salmon louse molecular toolbox to also include precise genome editing tools such as CRISPR/Cas9, the pace of identifying potential targets for chemical treatments, vaccine antigens, as well as expanding the understanding of parasite host interactions, could be increased. CRISPR/Cas9 and similar technologies are also proving to be versatile and technologies such as base editing and prime editing are emerging as viable options in salmon louse if the basic genome editing tool is functional.

The challenge of further increase food production and fish welfare in salmonid farms, without damaging the wild anadromous salmonid populations and other organisms, more knowledge about the salmon louse and its host interactions is crucial. With the emerging challenge of persistent reduction of wild salmonid population sizes and increase in salmon louse resistance to chemical treatments, combined with the increased cost related to salmon louse, the problem is ripe for a solution.

References

- ABOLOFIA, J., ASCHE, F. & WILEN, J. E. 2017. The Cost of Lice: Quantifying the Impacts of Parasitic Sea Lice on Farmed Salmon. *Marine Resource Economics*, 32, 329-349. DOI:10.1086/691981
- ALBERTS, B. 2014. *Molecular Biology of the Cell*, New York and Abingdon, UK, Garland Science.
- ANDERSEN, S. O. 2010. Insect cuticular sclerotization: A review. *Insect Biochemistry and Molecular Biology*, 40, 166-178. DOI:https://doi.org/10.1016/j.ibmb.2009.10.007
- BADAWY, A. A. B. 2017. Kynurenine Pathway of Tryptophan Metabolism: Regulatory and Functional Aspects. *International journal of tryptophan research : IJTR*, 10, 1178646917691938-1178646917691938. DOI:10.1177/1178646917691938
- BARKER, S. E., BRICKNELL, I. R., COVELLO, J., PURCELL, S., FAST, M. D., WOLTERS, W. & BOUCHARD, D. A. 2019. Sea lice, *Lepeophtheirus salmonis* (Krøyer 1837), infected Atlantic salmon (*Salmo salar* L.) are more susceptible to infectious salmon anemia virus. *PLoS one*, 14, e0209178-e0209178. DOI:10.1371/journal.pone.0209178
- BHATTACHARJEE, S., ROCHE, B. & MARTIENSSEN, R. A. 2019. RNA-induced initiation of transcriptional silencing (RITS) complex structure and function. *RNA biology*, 16, 1133-1146. DOI:10.1080/15476286.2019.1621624
- BJØRN, P. A., FINSTAD, B. & KRISTOFFERSEN, R. 2001. Salmon lice infection of wild sea trout and Arctic char in marine and freshwaters: the effects of salmon farms. *Aquaculture Research*, 32, 947-962. DOI:https://doi.org/10.1046/j.1365-2109.2001.00627.x
- BRADEN, L., MICHAUD, D., IGBOELI, O. O., DONDRUP, M., HAMRE, L., DALVIN, S., PURCELL, S. L., KONGSHAUG, H., EICHNER, C., NILSEN, F. & FAST, M. D. 2020. Identification of critical enzymes in the salmon louse chitin synthesis pathway as revealed by RNA interference-mediated abrogation of infectivity. *International Journal for Parasitology*, 50, 873-889. DOI:https://doi.org/10.1016/j.ijpara.2020.06.007
- BRANDAL, P. L. & EGIDIUS, E. 1977. Preliminary report on oral treatment against salmon lice, *Lepeophtheirus salmonis*, with Neguvon. *Aquaculture*, 10, 177-178. DOI:https://doi.org/10.1016/0044-8486(77)90019-9
- BØHN, T., GJELLAND, K. Ø., SERRA-LLINARES, R. M., FINSTAD, B., PRIMICERIO, R., NILSEN, R., KARLSEN, Ø., SANDVIK, A. D., SKILBREI, O. T. & ELVIK, K. M. S. 2020. Timing is everything: Survival of Atlantic salmon *Salmo salar* postsmolts during events of high salmon lice densities. *Journal of Applied Ecology*, 57, 1149-1160. DOI:https://doi.org/10.1111/1365-2664.13612
- CHRISTIE, A. E., FONTANILLA, T. M., RONCALLI, V., CIESLAK, M. C. & LENZ, P. H. 2014. Identification and developmental expression of the enzymes responsible for dopamine, histamine, octopamine and serotonin biosynthesis in the copepod crustacean *Calanus finmarchicus*. *General and Comparative Endocrinology*, 195, 28-39. DOI:https://doi.org/10.1016/j.ygcen.2013.10.003
- CIECHANOWSKA, K., POKORNOWSKA, M. & KURZYŃSKA-KOKORNIK, A. 2021. Genetic Insight into the Domain Structure and Functions of Dicer-Type Ribonucleases. *International Journal of Molecular Sciences*, 22, 616. DOI:https://doi.org/10.3390/ijms22020616
- COOPER, A. M. W., SILVER, K., ZHANG, J., PARK, Y. & ZHU, K. Y. 2018. Molecular mechanisms influencing efficiency of RNA interference in insects. *Pest Management Science*, 75, 18-28. DOI:https://doi.org/10.1002/ps.5126
- COSTELLO, M. J. 2006. Ecology of sea lice parasitic on farmed and wild fish. *Trends in Parasitology*, 22, 475-483. DOI:https://doi.org/10.1016/j.pt.2006.08.006

- COSTELLO, M. J. 2009. The global economic cost of sea lice to the salmonid farming industry. *Journal of Fish Diseases*, 32, 115-118.
DOI:<https://doi.org/10.1111/j.1365-2761.2008.01011.x>
- CRAWFORD, K., DIAZ QUIROZ, J. F., KOENIG, K. M., AHUJA, N., ALBERTIN, C. B. & ROSENTHAL, J. J. C. 2020. Highly Efficient Knockout of a Squid Pigmentation Gene. *Current Biology*, 30, 3484-3490.e4.
DOI:<https://doi.org/10.1016/j.cub.2020.06.099>
- CRONIN, T. W. & JINKS, R. N. 2001. Ontogeny of Vision in Marine Crustaceans. *American Zoologist*, 41, 1098-1107. DOI:<https://doi.org/10.1093/icb/41.5.1098>
- DALVIN, S., FROST, P., BIERING, E., HAMRE, L. A., EICHNER, C., KROSSØY, B. & NILSEN, F. 2009. Functional characterisation of the maternal yolk-associated protein (LsYAP) utilising systemic RNA interference in the salmon louse (*Lepeophtheirus salmonis*) (Crustacea: Copepoda). *International Journal for Parasitology*, 39, 1407-1415. DOI:<https://doi.org/10.1016/j.ijpara.2009.04.004>
- DAUBNER, S. C., LE, T. & WANG, S. 2011. Tyrosine hydroxylase and regulation of dopamine synthesis. *Archives of biochemistry and biophysics*, 508, 1-12.
DOI:[10.1016/j.abb.2010.12.017](https://doi.org/10.1016/j.abb.2010.12.017)
- DAWSON, L. H. J., PIKE, A. W., HOULIHAN, D. F. & MCVICAR, A. H. 1997. Comparison of the susceptibility of sea trout (*Salmo trutta* L.) and Atlantic salmon (*Salmo salar* L.) to sea lice (*Lepeophtheirus salmonis* (Krøyer, 1837)) infections. *ICES Journal of Marine Science*, 54, 1129-1139. DOI:[10.1016/S1054-3139\(97\)80018-5](https://doi.org/10.1016/S1054-3139(97)80018-5)
- DESJARDINS, P. & CONKLIN, D. 2010. NanoDrop microvolume quantitation of nucleic acids. *JoVE (Journal of Visualized Experiments)*, e2565. DOI:[10.3791/2565](https://doi.org/10.3791/2565)
- DONTSOV, A. E., FEDOROVICH, I. B., LINDSTRÖM, M. & OSTROVSKY, M. A. 1999. Comparative study of spectral and antioxidant properties of pigments from the eyes of two *Mysis relicta* (Crustacea, Mysidacea) populations, with different light damage resistance. *Journal of Comparative Physiology B*, 169, 157-164.
DOI:<https://doi.org/10.1007/s003600050206>
- DONTSOV, A. E., SAKINA, N. L., YAKOVLEVA, M. A., BASTRAKOV, A. I., BASTRAKOVA, I. G., ZAGORINSKY, A. A., USHAKOVA, N. A., FELDMAN, T. B. & OSTROVSKY, M. A. 2020. Ommochromes from the Compound Eyes of Insects: Physicochemical Properties and Antioxidant Activity. *Biochemistry (Moscow)*, 85, 668-678.
DOI:[10.1134/S0006297920060048](https://doi.org/10.1134/S0006297920060048)
- EFIMOV, I., BASRAN, J., THACKRAY, S. J., HANDA, S., MOWAT, C. G. & RAVEN, E. L. 2011. Structure and Reaction Mechanism in the Heme Dioxygenases. *Biochemistry*, 50, 2717-2724. DOI:[10.1021/bi101732n](https://doi.org/10.1021/bi101732n)
- EICHNER, C., DALVIN, S., SKERN-MAURITZEN, R., MALDE, K., KONGSHAUG, H. & NILSEN, F. 2015a. Characterization of a novel RXR receptor in the salmon louse (*Lepeophtheirus salmonis*, Copepoda) regulating growth and female reproduction. *BMC Genomics*, 16, 81. DOI:[10.1186/s12864-015-1277-y](https://doi.org/10.1186/s12864-015-1277-y)
- EICHNER, C., HAMRE, L. A. & NILSEN, F. 2015b. Instar growth and molt increments in *Lepeophtheirus salmonis* (Copepoda: Caligidae) chalimus larvae. *Parasitology International*, 64, 86-96. DOI:<https://doi.org/10.1016/j.parint.2014.10.006>
- EICHNER, C., HARASIMCZUK, E., NILSEN, F., GROTMOL, S. & DALVIN, S. 2015c. Molecular characterisation and functional analysis of LsChi2, a chitinase found in the salmon louse (*Lepeophtheirus salmonis*, Krøyer 1838). *Experimental Parasitology*, 151-152, 39-48.
DOI:<https://doi.org/10.1016/j.exppara.2015.01.011>
- EICHNER, C., NILSEN, F., GROTMOL, S. & DALVIN, S. 2014. A method for stable gene knock-down by RNA interference in larvae of the salmon louse (*Lepeophtheirus salmonis*). *Experimental Parasitology*, 140, 44-51.
DOI:<https://doi.org/10.1016/j.exppara.2014.03.014>
- EICHNER, C., ØVERGÅRD, A.-C., NILSEN, F. & DALVIN, S. 2015d. Molecular characterization and knock-down of salmon louse (*Lepeophtheirus salmonis*) prostaglandin E synthase. *Experimental Parasitology*, 159, 79-93.
DOI:<https://doi.org/10.1016/j.exppara.2015.09.001>

- FAIRCHILD, W., DOE, K., JACKMAN, P., ARSENAULT, J., AUBÉ, J., LOSIER, M. & COOK, A. 2010. Acute and chronic toxicity of two formulations of the pyrethroid pesticide deltamethrin to an amphipod, sand shrimp and lobster larvae. *Canadian Technical Report of Fisheries and Aquatic Sciences*, 2876, 34p.
- FAST, M. D., ROSS, N. W., MUISE, D. M. & JOHNSON, S. C. 2006. Differential Gene Expression in Atlantic Salmon Infected with *Lepeophtheirus salmonis*. *Journal of Aquatic Animal Health*, 18, 116-127. DOI:<https://doi.org/10.1577/H05-043.1>
- FIGON, F. & CASAS, J. 2019. Ommochromes in invertebrates: biochemistry and cell biology. *Biological Reviews*, 94, 156-183. DOI: <https://doi.org/10.1111/brv.12441>
- FIRE, A., XU, S., MONTGOMERY, M. K., KOSTAS, S. A., DRIVER, S. E. & MELLO, C. C. 1998. Potent and specific genetic interference by double-stranded RNA in *Caenorhabditis elegans*. *Nature*, 391, 806-811. DOI:10.1038/35888
- FORSKRIFT OM LAKSELUSBKJEMPELSE 2012. Forskrift om bekjempelse av lakselus i akvakulturanlegg.
- FROST, P. & NILSEN, F. 2003. Validation of reference genes for transcription profiling in the salmon louse, *Lepeophtheirus salmonis*, by quantitative real-time PCR. *Veterinary Parasitology*, 118, 169-174. DOI:<https://doi.org/10.1016/j.vetpar.2003.09.020>
- FUTAHASHI, R. & FUJIWARA, H. 2005. Melanin-synthesis enzymes coregulate stage-specific larval cuticular markings in the swallowtail butterfly, *Papilio xuthus*. *Development Genes and Evolution*, 215, 519-529. DOI:10.1007/s00427-005-0014-y
- GAMIL, A. A., GADAN, K., GISLEFOSS, E. & EVENSEN, Ø. 2020. Sea Lice (*Lepeophtheirus salmonis*) Infestation Reduces the Ability of Peripheral Blood Monocytic Cells (PBMCs) to Respond to and Control Replication of Salmonid Alphavirus in Atlantic Salmon (*Salmo salar* L.). *Viruses*, 12, 1450. DOI:<https://doi.org/10.3390/v12121450>
- GODWIN, S. C., DILL, L. M., REYNOLDS, J. D. & KRKOŠEK, M. 2015. Sea lice, sockeye salmon, and foraging competition: lousy fish are lousy competitors. *Canadian Journal of Fisheries and Aquatic Sciences*, 72, 1113-1120. DOI:<https://doi.org/10.1139/cjfas-2014-0284>
- GORMAN, M. J. & ARAKANE, Y. 2010. Tyrosine hydroxylase is required for cuticle sclerotization and pigmentation in *Tribolium castaneum*. *Insect Biochemistry and Molecular Biology*, 40, 267-273. DOI:<https://doi.org/10.1016/j.ibmb.2010.01.004>
- GOSTNER, J. M., GEISLER, S., STONIG, M., MAIR, L., SPERNER-UNTERWEGER, B. & FUCHS, D. 2020. Tryptophan metabolism and related pathways in psychoneuroimmunology: the impact of nutrition and lifestyle. *Neuropsychobiology*, 79, 89-99. DOI:<https://doi.org/10.1159/000496293>
- GREFSRUD, E. S., SVÅSAND, T., GLOVER, K., HUSA, V., HANSEN, P. K., SAMUELSEN, O. B., SANDLUND, N. & STIEN, L. H. 2019. Risikorapport norsk fiskeoppdrett 2019 - Miljøeffekter av lakseoppdrett. *Fisken og havet*.
- GURAGAIN, P., SPORSHEIM, B., SKJESOL, A., BÅTNES, A. S., OLSEN, Y., BONES, A. M. & WINGE, P. 2020. Phenylalanine Hydroxylase RNAi Knockdown Negatively Affects Larval Development, Molting and Swimming Performance of Salmon Lice. *Frontiers in Marine Science*, 7. DOI:10.3389/fmars.2020.608463
- HAMRE, L. A., EICHNER, C., CAIPANG, C. M. A., DALVIN, S. T., BRON, J. E., NILSEN, F., BOXSHALL, G. & SKERN-MAURITZEN, R. 2013. The Salmon Louse *Lepeophtheirus salmonis* (Copepoda: Caligidae) Life Cycle Has Only Two Chalimus Stages. *PLOS ONE*, 8, e73539. DOI:10.1371/journal.pone.0073539
- HAMRE, L. A., GLOVER, K. A. & NILSEN, F. 2009. Establishment and characterisation of salmon louse (*Lepeophtheirus salmonis* (Krøyer 1837)) laboratory strains. *Parasitology International*, 58, 451-460. DOI:<https://doi.org/10.1016/j.parint.2009.08.009>
- HANNA, M. E., BEDNÁŘOVÁ, A., RAKSHIT, K., CHAUDHURI, A., O'DONNELL, J. M. & KRISHNAN, N. 2015. Perturbations in dopamine synthesis lead to discrete physiological effects and impact oxidative stress response in *Drosophila*. *Journal of insect physiology*, 73, 11-19. DOI:10.1016/j.jinsphys.2015.01.001

- HARÐARDÓTTIR, H. M., MALE, R., NILSEN, F., EICHNER, C., DONDRUP, M. & DALVIN, S. 2019. Chitin synthesis and degradation in *Lepeophtheirus salmonis*: Molecular characterization and gene expression profile during synthesis of a new exoskeleton. *Comparative Biochemistry and Physiology Part A: Molecular & Integrative Physiology*, 227, 123-133.
DOI:https://doi.org/10.1016/j.cbpa.2018.10.008
- HELLEMANS, J., MORTIER, G., DE PAEPE, A., SPELEMAN, F. & VANDESOMPELE, J. 2007. qBase relative quantification framework and software for management and automated analysis of real-time quantitative PCR data. *Genome biology*, 8, 1-14.
DOI:10.1186/gb-2007-8-2-r19
- HOWE, K. L., ACHUTHAN, P., ALLEN, J., ALLEN, J., ALVAREZ-JARRETA, J., AMODE, M. R., ARMEAN, I. M., AZOV, A. G., BENNETT, R., BHAI, J., BILLIS, K., BODDU, S., CHARKHCHI, M., CUMMINS, C., DA RIN FIORETTO, L., DAVIDSON, C., DODIYA, K., EL HOUDAIGUI, B., FATIMA, R., GALL, A., GARCIA GIRON, C., GREGO, T., GUIJARRO-CLARKE, C., HAGGERTY, L., HEMROM, A., HOURLIER, T., IZUOGU, O. G., JUETTEMANN, T., KAIKALA, V., KAY, M., LAVIDAS, I., LE, T., LEMOS, D., GONZALEZ MARTINEZ, J., MARUGÁN, J. C., MAUREL, T., MCMAHON, A. C., MOHANAN, S., MOORE, B., MUFFATO, M., OHEH, D. N., PARASCHAS, D., PARKER, A., PARTON, A., PROSOVETSKAIA, I., SAKTHIVEL, M. P., SALAM, AHAMED I A., SCHMITT, B. M., SCHUILENBURG, H., SHEPPARD, D., STEED, E., SZPAK, M., SZUBA, M., TAYLOR, K., THORMANN, A., THREADGOLD, G., WALTS, B., WINTERBOTTOM, A., CHAKIACHVILI, M., CHAUBAL, A., DE SILVA, N., FLINT, B., FRANKISH, A., HUNT, S. E., IISLEY, G. R., LANGRIDGE, N., LOVELAND, J. E., MARTIN, F. J., MUDGE, J. M., MORALES, J., PERRY, E., RUFFIER, M., TATE, J., THYBERT, D., TREVANION, S. J., CUNNINGHAM, F., YATES, A. D., ZERBINO, D. R. & FLICEK, P. 2020. Ensembl 2021. *Nucleic Acids Research*, 49, D884-D891.
DOI:10.1093/nar/gkaa942
- IGBOELI, O. O., BURKA, J. F. & FAST, M. D. 2014. *Lepeophtheirus salmonis*: a persisting challenge for salmon aquaculture. *Animal Frontiers*, 4, 22-32.
DOI:10.2527/af.2014-0004
- IVERSEN, A., HERMANSEN, Ø., NYSTØYL, R., HESS, E. J., ROLLAND, K. H., GARSHOL, L. D. & MARTHINUSSEN, A. 2019. Kostnadsutvikling og forståelse av drivkrefter i norsk lakseoppdrett. Nofima rapportserie 35/2019. *Tromsø: Nofima AS*.
- KOMISARCZUK, A. Z., KONGSHAUG, H. & NILSEN, F. 2018. Gene silencing reveals multiple functions of Na⁺/K⁺-ATPase in the salmon louse (*Lepeophtheirus salmonis*). *Experimental Parasitology*, 185, 79-91.
DOI:https://doi.org/10.1016/j.exppara.2018.01.005
- KRKOŠEK, M., CONNORS, B. M., MORTON, A., LEWIS, M. A., DILL, L. M. & HILBORN, R. 2011. Effects of parasites from salmon farms on productivity of wild salmon. *Proceedings of the National Academy of Sciences*, 108, 14700-14704.
DOI:https://doi.org/10.1073/pnas.1101845108
- KRKOSEK, M., LEWIS, M. A. & VOLPE, J. P. 2005. Transmission dynamics of parasitic sea lice from farm to wild salmon. *Proceedings. Biological sciences*, 272, 689-696.
DOI:10.1098/rspb.2004.3027
- KRØYER, H. N. 1837. *De Danske Østersbanker, et Bidrag til Kundskab om Danmarks Fiskerier*, Copenhagen, Denmark, S. Triers officin.
- KUMAR, S., STECHER, G. & TAMURA, K. 2016. MEGA7: Molecular Evolutionary Genetics Analysis Version 7.0 for Bigger Datasets. *Molecular Biology and Evolution*, 33, 1870-1874. DOI:10.1093/molbev/msw054
- LAXMYR, L. 1985. Tyrosine hydroxylase activity in the central nervous system of the crayfish, *Pacifastacus leniusculus* (Crustacea, Decapoda). *Journal of Comparative Physiology B*, 155, 603-609. DOI:https://doi.org/10.1007/BF00694451
- LINDBO, J. A. & DOUGHERTY, W. G. 1992. Untranslatable transcripts of the tobacco etch virus coat protein gene sequence can interfere with tobacco etch virus replication in transgenic plants and protoplasts. *Virology*, 189, 725-33. DOI:10.1016/0042-6822(92)90595-g

- LISOWIEC-WĄCHNICKA, J., BARTYŚ, N. & PASTERNAK, A. 2019. A systematic study on the influence of thermodynamic asymmetry of 5'-ends of siRNA duplexes in relation to their silencing potency. *Scientific Reports*, 9, 2477. DOI:10.1038/s41598-018-36620-9
- LLEWELLYN, M. S., LEADBEATER, S., GARCIA, C., SYLVAIN, F. E., CUSTODIO, M., ANG, K. P., POWELL, F., CARVALHO, G. R., CREER, S., ELLIOT, J. & DEROME, N. 2017. Parasitism perturbs the mucosal microbiome of Atlantic Salmon. *Scientific Reports*, 7, 43465. DOI:10.1038/srep43465
- LONG, A., GARVER, K. A. & JONES, S. R. M. 2019. Synergistic osmoregulatory dysfunction during salmon lice (*Lepeophtheirus salmonis*) and infectious hematopoietic necrosis virus co-infection in sockeye salmon (*Oncorhynchus nerka*) smolts. *Journal of fish diseases*, 42, 869-882. DOI:10.1111/jfd.12989
- LUO, Y., NA, Z. & SLAVOFF, S. A. 2018. P-Bodies: Composition, Properties, and Functions. *Biochemistry*, 57, 2424-2431. DOI:10.1021/acs.biochem.7b01162
- MAGES, P. A. & DILL, L. M. 2010. The effect of sea lice (*Lepeophtheirus salmonis*) on juvenile pink salmon (*Oncorhynchus gorbuscha*) swimming endurance. *Canadian Journal of Fisheries and Aquatic Sciences*, 67, 2045-2051. DOI:https://doi.org/10.1139/F10-121
- MAPANAO, R., CHANG, C.-C. & CHENG, W. 2017. The upregulation of immune responses in tyrosine hydroxylase (TH) silenced *Litopenaeus vannamei*. *Developmental & Comparative Immunology*, 67, 30-42. DOI:https://doi.org/10.1016/j.dci.2016.11.002
- MORTON, A., ROUTLEDGE, R., PEET, C. & LADWIG, A. 2004. Sea lice (*Lepeophtheirus salmonis*) infection rates on juvenile pink (*Oncorhynchus gorbuscha*) and chum (*Oncorhynchus keta*) salmon in the nearshore marine environment of British Columbia, Canada. *Canadian Journal of Fisheries and Aquatic Sciences*, 61, 147-157. DOI:https://doi.org/10.1139/f04-016
- NICHOLAS, K. & NICHOLAS, H. GeneDoc: a tool for editing and annotating multiple sequence alignments. 1997.
- NORWEGIAN BIODIVERSITY INFORMATION CENTRE. 2021. *Innsyn i foreløpig vurdering til Rødlista for arter 2021: Laks Salmo salar Linnaeus, 1758* [Online]. Available: <https://innsyn.artsdatabanken.no/artsrapport/tilbakemelding/8149> [Accessed March 30 2021].
- O'DONOHUE, P., KANE, F., MCDERMOTT, T. & JACKSON, D. 2016. Sea reared rainbow trout *Oncorhynchus mykiss* need fewer sea lice treatments than farmed Atlantic salmon *Salmo salar*. *Bull. Eur. Ass. Fish Pathol*, 36, 2016.
- PARSONS, A. E., ESCOBAR-LUX, R. H., SÆVIK, P. N., SAMUELSEN, O. B. & AGNALT, A.-L. 2020. The impact of anti-sea lice pesticides, azamethiphos and deltamethrin, on European lobster (*Homarus gammarus*) larvae in the Norwegian marine environment. *Environmental Pollution*, 264, 114725. DOI:https://doi.org/10.1016/j.envpol.2020.114725
- PONZONI, S. 2014. Tyrosine hydroxylase protein expression in ventral nerve cord of Neotropical freshwater crab. *Tissue and Cell*, 46, 482-489. DOI:https://doi.org/10.1016/j.tice.2014.08.007
- PONZONI, S. 2017. Manganese tissue accumulation and tyrosine hydroxylase immunostaining response in the Neotropical freshwater crab, *Dilocarcinus pagei*, exposed to manganese. *Invertebrate Neuroscience*, 17, 5. DOI: 10.1007/s10158-017-0198-7
- RSTUDIO TEAM 2020. RStudio: Integrated Development for R. RStudio, PBC, Boston, MA.
- SAMSING, F., OPPEDAL, F., DALVIN, S., JOHNSEN, I., VÅGSETH, T. & DEMPSTER, T. 2016. Salmon lice (*Lepeophtheirus salmonis*) development times, body size, and reproductive outputs follow universal models of temperature dependence. *Canadian Journal of Fisheries and Aquatic Sciences*, 73, 1841-1851. DOI:10.1139/cjfas-2016-0050
- SANDLUND, L., NILSEN, F., MALE, R. & DALVIN, S. 2016. The ecdysone receptor (EcR) is a major regulator of tissue development and growth in the marine salmonid ectoparasite, *Lepeophtheirus salmonis* (Copepoda, Caligidae). *Molecular and*

- Biochemical Parasitology*, 208, 65-73.
DOI:<https://doi.org/10.1016/j.molbiopara.2016.06.007>
- SCHLEE, M. & HARTMANN, G. 2016. Discriminating self from non-self in nucleic acid sensing. *Nature Reviews Immunology*, 16, 566-580. DOI:10.1038/nri.2016.78
- SCHNEIDER, C. A., RASBAND, W. S. & ELICEIRI, K. W. 2012. NIH Image to ImageJ: 25 years of image analysis. *Nature methods*, 9, 671-675. DOI:10.1038/nmeth.2089
- SCHRAM, T. A. 1993. Supplementary descriptions of the developmental stages of *Lepeophtheirus salmonis* (Krøyer, 1837)(Copepoda: Caligidae). In: BOXSHALL, G. A. & DEFAYE, D. (eds.) *Pathogens of Wild and Farmed Fish: Sea Lice*. Devon, Great Britain: NHBS - Ellis Horwood.
- SHEPHARD, S., MACINTYRE, C. & GARGAN, P. 2016. Aquaculture and environmental drivers of salmon lice infestation and body condition in sea trout. *Aquaculture Environment Interactions*, 8, 597-610. DOI:10.3354/aei00201
- SONG, Y., VILLENEUVE, D. L., TOYOTA, K., IGUCHI, T. & TOLLEFSEN, K. E. 2017. Ecdysone receptor agonism leading to lethal molting disruption in arthropods: review and adverse outcome pathway development. *Environmental science & technology*, 51, 4142-4157. DOI:10.1021/acs.est.7b00480
- THORSTAD, E. B., FORSETH, T. & FISKE, P. 2020. Status for norske laksebestander i 2020. *Vitenskapelig råd for lakseforvaltning*.
- TORRISSEN, O., JONES, S., ASCHE, F., GUTTORMSEN, A., SKILBREI, O. T., NILSEN, F., HORSBERG, T. E. & JACKSON, D. 2013. Salmon lice-impact on wild salmonids and salmon aquaculture. *Journal of fish diseases*, 36, 171-194.
DOI:<https://doi.org/10.1111/jfd.12061>
- TRUE, J. R., EDWARDS, K. A., YAMAMOTO, D. & CARROLL, S. B. 1999. Drosophila wing melanin patterns form by vein-dependent elaboration of enzymatic prepatterns. *Current Biology*, 9, 1382-1391. DOI:[https://doi.org/10.1016/S0960-9822\(00\)80083-4](https://doi.org/10.1016/S0960-9822(00)80083-4)
- TRÖBE, C., KONGSHAUG, H., DONDRUP, M. & NILSEN, F. 2015. Characterisation of iron regulatory protein 1A and 1B in the blood-feeding copepod *Lepeophtheirus salmonis*. *Experimental Parasitology*, 157, 1-11.
DOI:<https://doi.org/10.1016/j.exppara.2015.06.010>
- TRÖBE, C., NILSEN, F. & DALVIN, S. 2014. RNA interference mediated knockdown of the KDEL receptor and COPB2 inhibits digestion and reproduction in the parasitic copepod *Lepeophtheirus salmonis*. *Comparative Biochemistry and Physiology Part B: Biochemistry and Molecular Biology*, 170, 1-9.
DOI:<https://doi.org/10.1016/j.cbpb.2013.12.006>
- TUCCA, F., DÍAZ-JARAMILLO, M., CRUZ, G., SILVA, J., BAY-SCHMITH, E., CHIANG, G. & BARRA, R. 2014. Toxic effects of antiparasitic pesticides used by the salmon industry in the marine amphipod *Monocorophium insidiosum*. *Archives of environmental contamination and toxicology*, 67, 139-148. DOI:10.1007/s00244-014-0008-8
- WAGNER, G. N., MCKINLEY, R. S., BJØRN, P. A. & FINSTAD, B. 2003. Physiological impact of sea lice on swimming performance of Atlantic salmon. *Journal of Fish Biology*, 62, 1000-1009. DOI:<https://doi.org/10.1046/j.1095-8649.2003.00091.x>
- WICKHAM, H. 2016. *ggplot2: Elegant Graphics for Data Analysis*, New York, Springer-Verlag.
- WILSON, C. H. & HARTLINE, D. K. 2011. Novel organization and development of copepod myelin. i. ontogeny. *Journal of Comparative Neurology*, 519, 3259-3280.
DOI:<https://doi.org/10.1002/cne.22695>
- WILSON, R. C. & DOUDNA, J. A. 2013. Molecular mechanisms of RNA interference. *Annual review of biophysics*, 42, 217-239. DOI:10.1146/annurev-biophys-083012-130404
- ZHANG, Y., KANG, S. A., MUKHERJEE, T., BALE, S., CRANE, B. R., BEGLEY, T. P. & EALICK, S. E. 2007. Crystal Structure and Mechanism of Tryptophan 2,3-Dioxygenase, a Heme Enzyme Involved in Tryptophan Catabolism and in Quinolate Biosynthesis. *Biochemistry*, 46, 145-155. DOI:10.1021/bi0620095

Appendices

List of appendices

Appendix 1: *LsPale* and *LsTDO* transcripts

Appendix 2: Amino acid sequences used for phylogenetic analysis and protein alignment

Appendix 3: qPCR setup

Appendix 4: Primers used for PCR, qPCR, and sequencing

Appendix 5: PCR setup

Appendix 6: Gel electrophoresis setup

Appendix 7: pCRTM4-TOPO[®] TA cloning vector map

Appendix 8: Recipe for Luria Bertani media

Appendix 9: *Arabidopsis thaliana* LRK sequence with T7 promoter

Appendix 1: *LsPale* and *LsTDO* transcripts

The transcripts of *LsPale* and *LsTDO* on FASTA-format. Template used for dsRNA synthesis is highlighted in blue and primer sites for addition of T7 promoter is in bold. The primers are listed in Appendix 4.

>*LsPale*_1876bp

```
TATATCCAGATATTATAATCCAAATTAAGTTCTGAACACCCACATTTTTTGCAGAATTC
AAGTCCCTAGGACGTACTCCATAGTCAAAATTAAGCAAATTTTCAAAAACAAGGTTGAGG
GTGTTTTAACCCTAACTAAAACTTTTTCTCAACTTGGTCGAAAGATATATAGATATAACG
ACGAAGAAGGAGAATTTGCTTCAAAAAGTATGCACAAAGAAATAGAGGATACCGTAGTGG
AGGAAAACAATCCGTTATGATGGACACTCGAGGTAATCGAGAAAAGTTTGCTATCAATA
AATCATATAGTATTGAGAATGGCTATGGTAGATCTACACGGAGTTTAGTAGGGGATGCAA
AGTTTGAGACCCTTGTGCGTAAGGAAACAAAACCTTTCTCTTCTAGAAAACATTAAGAAAC
AAAATAAAGAGTCAACGTTAGAGGAACTTTGTAACGAGGACATATCTTTACTTGAATCTG
TTCTCTGCACAAATGAAAACAGAGAAAATGATAAAAATTAATAATTTTACTTCTTTGTG
GAGTCAAGGATCCTGTATCTGAGTGTATCAATAATATTATCGAGCATGTATCTGAAATGG
ATGGAGAATTGACTCATTTAGAGACAAGAACTCTGCCACGTTTCTATCTTTTACGGATG
TACTCTTAAAGTTTGTGTTTCAAGAAAATAAAGTTGGGGATCTTATCATGCAAATTCGAG
GACTACCTCCGGTTCAAAGATTGAACATTCTTCTGCTGGACGATCCGTGGATGCCAAATTCG
CGTGGTTTTCTCGACATATTGCCGAATTAGATCAATGCAATCATCTAATAACTAAATTTG
AGCCTGAATTGGATATGGAACATCCTGGATGGTCGGATCCAGTATATCGACAGAGAAGGA
AGGATATTGCAGAAATATCTTTAATTACAAATATGGAGAACCGATTCTTGTGTAACAT
ATGCAGAAGATGAGATAAAAAGCCTGGGGAGCTGTCTATAAAAAAGTAAAGGAATTAATAA
ATGGAAGAGCTTGCAGTATTCATCGTCATGCCTTTGAAAAGATGCAGGAAGATCTTGGAA
TGTCTGAGAATAGTATCCCTCAACTGGAAAATGTCTCCAAATTCCTACAAAGATCTTCAG
GGTTTACACTAAGGCCTGCTGCTGGACTAGTGACTGCAAGAGATTTTTTGGCAAGTCTAG
CCTTTAGAGTGTTCATGTACACAATATATCCGGCATGGCTCTCAACCTCATCATTTCTC
CAGAACCAGATCTGATACATGAGCTCCTCGGACATTGTGCAATGTTTGCAAATAAAGAGT
TTGCTCAATTTTTCTCAAGAGATTGGACTTGCTCTCGGATCCACAGATGAAGAAAATG
AAAAATTAGCAACATTTGACTGGTTTACTGTGGAGTTTGGCCTCTGTAAGGAAAATGGAG
CAATACGAGCATATGGAGCTGGGTTGTTGTCCAGCTACGGCGAGCTTTTGCATTCTTAT
CGGATGAACCAGAAAAAGAGATTTCAATCCCCTGTAGCATGTCTGACTGAGTACGACG
ATCAGGCATACCAATCGATTTACTACGTAGCAGAGAGCTTTGAGGATGCACCTTGAAAAGT
TTAGACGATGGGTCAACATGAATTTGACTCGACCCGTGGAAAATGCGATATTGCCCGTATA
CACAAAGAGTCAAGTTTTTGGACTCTGTCCAAGGGATGGAAAACCTTAGTCACAGAAATGA
AAGTATCACTCAATCATTTGAATAATGCTTTTAGAAGAATTGAGAAGAAGTGAATCTTTC
CTATCAAACCTCAATACACTAAATGACTCTTAATTACAGAAAAGATGCACAGTACTTATTG
AAGAACAAAAAAAAC
```

>*LsTDO*_1534bp

```
GGGGGGTTTAGTTCAACTTCAACAACACTAACTAAAATGAATGGTAATGCTAGAATTGAAT
GTCCCTTTGCTGGTTTCATCATCGTCTCTTCTAACAAGAATCCTGATTCTGATAAAATACG
ATACAGAAAATGGAGTGCATTTGCTTAGTGATGAAGGAGGAAAGTCTTATGAGGATGTTT
TACAGCTCGAGATGGTTCTTAAGGCACAAAAAACCTACTCTGATGTACATGATGAACATT
TTTTATTATTATTCATCAAGTACATGAACCTCTGGTTTAAAGCAAATCCTGTCCGACATAA
ACTCCGTGATTGAGATGTTTTCAACTAAAAGAGAAAACGGATTTAGTGGATGAATCTCATA
TGAAGATTATCAACTCACGACTCTATAGGGTAGTGAGGATCCTTCGAAGCCTCGTAGACT
CCATTACTCTCCTTGAACAATGTCTCCATCTGATTTTTTAAACTTCCGTGATGTTCTTT
CTACTGCATCTGGATTTCAAAGCTATCAATTCGGTATGCTTGAGAATAAACTGGGACTCA
AAAAGGAAAATCGAATCAATATAACAAGTGCCATTATACGGAAGTCTTTGACTATAATC
CCGAATATAAGAAGGAACCTCAAGATGTGGAAACTTCTGATACTCTAAGCAGCAGCAGATTC
AAAAATGGCTGGAGAGAACACCTGGACTGGAAAAGGATGAATTTGACTTTATGAACAAGT
ATAAGGAGACAGTAAATGAAATATTGAAATCTGAAAAGGATAGCATTGACAAAATGTCCA
ATGCTTCCCGAAAAAATATTCCGTATCCTCTTTTCGAGACTCGTAAGATGCTCTTTGATT
CCATTTTTGAGGAGGAATTGCATAATATTCTCATGGCAAGAGGAGAAAAGACGTTTACAC
ACAAGGCCTTTTGTGGAGCTTTAATGATTAAATGTTATTCCGATGAGCCTCGCTTCCATC
AACCAATTCTCTTCTTGATCATTTGGCAACCATTGACTCTCTTTTAAACAAAATGGAGAT
ATAATCATGTCTCATGGTTCAAAGAATGTTGGGATCCCAACAACCTCGGCACGGGTGGCT
```

CAAGTGGATACACTTACCTACGAACAACCTCTAAGCGACAACCTACAAAATCTTCCTAGACT
TATTTAACCTCTCCACATTCATCATTCGTAAGGAGTACATCCCTAAACTCACTCCTGAGA
TGATATCCATTCTTCGTACTCATATCTAATGATTGCAGTCCAGGATGACATTTGATGATG
TCGAGATGCGAGTCCAGTACTTCTTCTTCTTATAATTACTCTCCCTTTTTATTAATTAAT
TATTTTCTCTCTTAAAATATCATGACGCCATTTATATTGATGATTGATATAACTTGTTTA
TGTCATTAATAATCAAATGTGTGGATGGAGGATTTTTCTTATTTTTTCATACATTATTCT
GACCTCTGATGTAAAATTTTGACTTACATTGTGCTGTAGATATTACGTACTTATACATAT
ATAATAGCAAGACTATAAATATAAAATAAAATGC

Appendix 2: Amino acid sequences used for phylogenetic analysis and protein alignment

Accession numbers to the amino acid sequences used for phylogenetic analysis and protein alignment are listed in supplementary table 2.1

Supplementary table 2.1: Tyrosine hydroxylase (TH) and tryptophan 2,3-dioxygenase (TDO) sequences used for phylogenetic analysis and alignment.

* Metagenomic copepod data from the MATOU Marine Atlas of Tara Oceans +metaG database (<https://tara-oceans.mio.osupytheas.fr/ocean-gene-atlas/>).

Protein	Accession number	Enzymatic activity
<i>Lepeophtheirus salmonis</i> TH (LsPale)	CDW39915.1, HACA01022554.1:547-1626	Tyrosine hydroxylase
<i>Eurytemora affinis</i> TH (EfTH)	XP_023337590.1	Tyrosine hydroxylase
<i>Harpegnathos saltator</i> TH (HsTH)	XP_025156819.1	Tyrosine hydroxylase
<i>Drosophila melanogaster</i> Pale (DmPale)	NP_476897.1	Tyrosine hydroxylase
<i>Xenopus laevis</i> th.S (Xl-th.S)	NP_001091392.1	Tyrosine hydroxylase
<i>Callorhinchus milii</i> Tyrosinase (CmTyrosinase)	XP_007902983.1	Tyrosine hydroxylase
<i>Danio rerio</i> th (Dr-th)	NP_571224.1	Tyrosine hydroxylase
<i>Homo sapiens</i> TH (HsTH)	NP_000351.2	Tyrosine hydroxylase
<i>Saccoglossus kowalevskii</i> TH (SKTH)	XP_006813567.1	Tyrosine hydroxylase
<i>Branchiostoma belcheri</i> TH (BbTH)	XP_019634110.1	Tyrosine hydroxylase
<i>Strongylocentrotus purpuratus</i> TH (SpTH)	XP_786206.1	Tyrosine hydroxylase
<i>Acanthaster planci</i> TH (ApTH)	XP_022079305.1	Tyrosine hydroxylase
<i>Caenorhabditis elegans</i> cat-2 (Ce-cat-2)	NP_001254009.1	Tyrosine hydroxylase
<i>Lepeophtheirus salmonis</i> TDO (LsTDO)	ACO12271.1	Tryptophan 2,3-dioxygenase
TARA Copepoda TDO (TARA-TDO)*	MATOU-v1_105733929	Tryptophan 2,3-dioxygenase
<i>Daphnia pulex</i> TDO (DpTDO)	EFX83853.1	Tryptophan 2,3-dioxygenase

<i>Drosophila melanogaster</i> vermillion (DmVermillion)	NP_511113.1	Tryptophan 2,3- dioxygenase
<i>Branchiostoma belcheri</i> TDO (BbTDO)	XP_019647219.1	Tryptophan 2,3- dioxygenase
<i>Saccoglossus kowalevskii</i> TDO (SkTDO)	XP_002732444.1	Tryptophan 2,3- dioxygenase
<i>Monosiga brevicollis</i> TDO (MbTDO)	XP_001748573.1	Tryptophan 2,3- dioxygenase
<i>Nematostella vectensis</i> TDO (NvTDO)	EDO49705.1	Tryptophan 2,3- dioxygenase
<i>Caenorhabditis elegans</i> tdo-2 (Ce- tdo-2)	NP_498284.1	Tryptophan 2,3- dioxygenase
<i>Danio rerio</i> TDO (DrTDO)	NP_956150.1	Tryptophan 2,3- dioxygenase
<i>Homo sapiens</i> TDO2 (HsTDO)	NP_005642.1	Tryptophan 2,3- dioxygenase

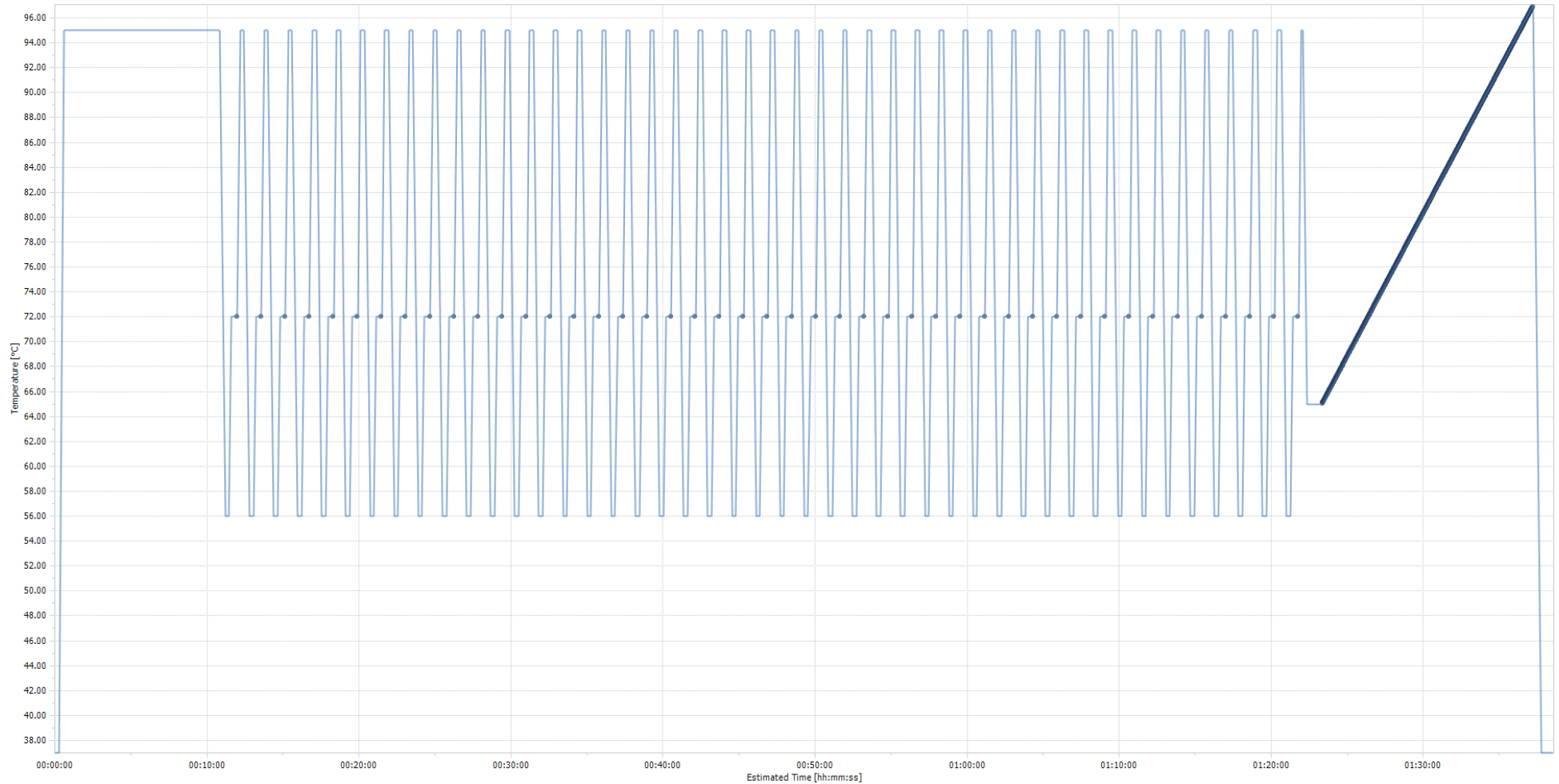
Appendix 3: qPCR setup

All reactants included in 20 μ L qPCR reactions are included in Supplementary table 3.1. Thermal setting for the LightCycler® 96 (Roche) is included in Supplementary figure 3.1.

Supplementary table 3.1: Reactants added in LightCycler® 480 Multiwell 96-well white plates (Roche) before qPCR analysis.

qPCR reaction setup	
Reactants	Volume (μL)
PCR-grader water	3
LightCycler® 480 SYBR Green I Master reaction mix (Roche)	10
Forward primer (5 μ M)	1
Reverse primer (5 μ M)	1
cDNA template	5
Final volume	20

Supplementary figure 3.1: Thermal settings for the LightCycler® 96 (Roche) when performing qPCR analysis. An initial 10-minute 95 °C preincubation was followed by 45 cycles of a three-step thermal cycling program (95 °C for 15s, 56 °C for 15s and 72 °C for 20s), with a fluorescence detection at the end of each cycle. After amplification, the temperature was increased to 95 °C for 5s, before it was lowered to 65 °C for 1 minute. The temperature was then ramped up by 2.2 °C/s to 97 °C, with continuous fluorescence detection. After denaturation, the temperature was lowered to 37 °C and the analysis complete.



Appendix 4: Primers used for PCR, qPCR, and sequencing

List of the primers used in all PCR and qPCR runs in this project are included in Supplementary table 4.1 and 4.2.

Supplementary table 4.1: PCR primers used for amplification or sequencing and their target genes.

* - T7 primers were designed to incorporate the T7 promoter according T7 RiboMAX™ Express RNAi System's technical bulletin. T7 promoter are in italic, and the full sequence added to the 5' of the amplicon are shown in brackets.

** - M13-primers were used with cloning vector as template or for sequencing

Name	Sequence (5'→3')	Target gene
LsPale_Fw	ATGATGGACACTCGAGGTAATC	<i>Ls Pale</i>
LsPale_Rw	AATCTTTGAACCGGAGGTAGTC	
LsTDO_Fw	AATTGAATGTCCCTTTGCTGGT	<i>Ls TDO</i>
T7_LsTDO_Fw*	[GGATCCTAATACGACTCACTATAGGN]- AATTGAATGTCCCTTTGCTGGT	
LsTDO_Rw	CTCAAGCATAACGGAATTGATAG	
T7_LsTDO_Rw*	[GGATCCTAATACGACTCACTATAGGN]- CTCAAGCATAACGGAATTGATAG	
M13 Forward	GTA AACGACGGCCAG	pCR®4-TOPO cloning vector
M13 Reverse	CAGGAAACAGCTATGAC	

Supplementary table 4.2: qPCR primers used for amplification and their target genes.

Name	Sequence (5'→3')	Target gene	Encoded protein
LsEF1a_Fw3	GGTCGACAGACGTACTGGTAAATCC	<i>LsEF1a</i>	Elongation factor 1 a
LsEF1a_Rw3	TGCGGCCTTGGTGGTGGTTC		
LsADT3_Fw	CTGGAGAGGGAATTTGGCTAACGTG	<i>LsADT3</i>	ADT, ATP carrier protein 3
LsADT3_Rw	ACCCTGGACACCGTCAGACTTCACG		
LsPale_q_Fw	GCAACATTGTA CTGGTTTACTG	<i>LsPale</i>	Tyrosine hydroxylase
LsPale_q_Rw	GTATGCCTGATCGTCGTA CTCA		
LsTDO_q_Fw	TGGATACTTACCTACGAACA	<i>LsTDO</i>	Tryptophan 2,3 dioxygenase
LsTDO_q_Rw	GATGTA CTCTTACGAATGATG		
LsPAH_eFw6	GAAATACGCCTGTGATGAATTC	<i>LsPAH</i>	Phenylalanine hydroxylase
LsPAH_eRw6	TTAAGAAGTCGGACACCTCTTG		

LsPNMT_Fw2	GTAGTAGGTTTCACTGATATGCC	<i>LsPNMT</i>	Phenylethanolamine- N-methyltransferase
LsPNMT_Rw2	GTTGAACACATCACAGGAGCTT		
LsDoH_Fw2	GAAGACTGATTTCAACAACATGC	<i>LsDOH</i>	Dopamine hydroxylase
LsDoH_Rw2	CTCCAGAGTTGTACTACACAT		
LsDDC_Fw1	GGCATCATCCAACTTTTACGC	<i>LsDDC</i>	DOPA decarboxylase
LsDDC_Rw1	GTGAGGCAATCCATGAAAATCC		
LsKMO_Fw4	CAACGATTCTTACCAGCAACTC	<i>LsKMO</i>	Kynurenine 3- monooxygenase
LsKMO_Rw2	CGAACACGACTTATTCCATCCA		
LsKF_F2	TTTAGAAATGGCTCAAAGGCTC	<i>LsKF</i>	Kynurenine formamidase
LsKF_R1	TTCTCCAACAATAACGTAGGCA		

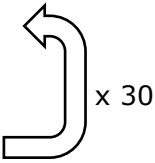
Appendix 5: PCR setup

All reactants included in 20 and 50 μL PCR reactions, as well as the thermal cycling steps and temperatures used for PCR, are included in supplementary table 5.1.

Supplementary table 5.1: PCR reaction setup and thermal cycles.

PCR reaction setup		
Reactants	Volume (μL) in 20 μL PCR-reaction	Volume (μL) in 50 μL PCR-reaction
dNTP	2	5
10x Buffer	2	5
5 μM forward primer	1	2.5
5 μM reverse primer	1	2.5
Taq polymerase	0.1	0.25
Nuclease-free water	11.9	29.75
DNA template	2	5
Final volume	20	50

Thermal cycles		
Step	Temperature ($^{\circ}\text{C}$)	Duration (min)
Initial melting	95	5
Melting	95	0.5
Annealing	Lowest primer T_m - 5	0.25
Elongation	72	0.5
Final elongation	72	5



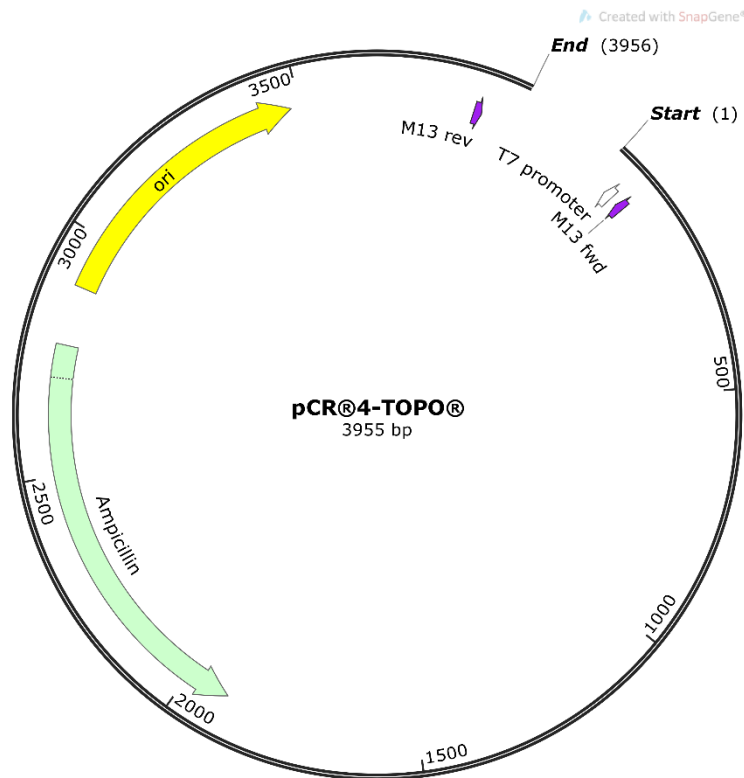
Appendix 6: Gel electrophoresis setup

Separation of DNA and RNA fragments by gel electrophoresis in 1% (w/v) agarose was done as follows:

- 1 g agarose and 99 ml 1x TAE buffer (4.84 g TRIZMA base, 1.142 ml glacial acetic acid, 2 ml EDTA (500 mM, pH 8)/L) was mixed and boiled in microwave until the agarose powder was completely dissolved.
- Gels were cast in a casting tray with a gel comb. Combs casting 8, 15 or 20 wells were used.
- 2 mL GelRed® (Sigma-Aldrich) per 100 mL agarose solution was also added.
- 50-300 µg of sample was loaded in individual wells. An equal amount of 1 Kb Plus DNA ladder (Invitrogen) was added to the wells flanking the samples.
- Gels were run on a PowerPac Basic® (Bio-Rad) in a two-step manner:
 1. An initial 20-minute 20 V step.
 2. A 70 V step for about 60 minutes.
- The gels were visualized under UV light in a G:BOX Chemi XRQ (Syngene)

Appendix 7: pCR™4-TOPO® TA cloning vector map

A map of the pCR™4-TOPO® TA cloning vector is included in Supplementary figure 7.1.



Supplementary figure 7.1: Map of the pCR⁴-TOPO cloning vector and its most relevant elements and features, including the T7 promoter and M13 primer sites, as well as ampicillin resistance and origin of replication (ori). Made with SnapGene® software (from Insightful Science; available at snappgene.com).

Appendix 8: Recipe for Luria Bertani media

Luria Bertani (LB) medium was used for bacterial growth on agar plates and in liquid cultures. Peptone, yeast extract and NaCl was added to MQ H₂O according to supplementary table 8.1 before the solution was mixed with until all solutes completely dissolved. The pH was then adjusted to 7 by adding sodium hydroxide (NaOH), and the volume was adjusted with MQ H₂O to the desired volume. The media was then autoclaved at 121 °C for 20 minutes.

For selective media, filter-sterile ampicillin was added to a concentration of 1µg/µL, after cooling the media to below 60 °C. For plates, agarose was added to the media before autoclaving, and plates were poured directly on a sterile bench.

Plates and liquid media were stored at 4 °C and at room temperature, respectively. Both were heated to 37 °C before use.

Supplementary table 8.1: all ingredients in Luria Bertani medium.

* Added when medium for plates was prepared. ** Added when selective medium was prepared.

Content	Amount
Peptone	10 g/L
Yeast extract	5 g/L
NaCl	10 g/L
MQ H ₂ O	950 g/L
Agarose *	15 g/L
Ampicillin (100 mg/L) **	1 µg/µL

Appendix 9: *Arabidopsis thaliana* LRK sequence with T7 promoter

FASTA-format of the *A. thaliana* LRK sequence used to synthesize the dsRNA used for the mock control treatments (dsCtrl).

>*A.thaliana_LRK_T7_sequence*

```
TGGCGTCTAGATACCCTCACTAAAGGGACTAGTCCTGCAGGTTTAAACGAATTCGCCCTTCCCCTACCTACCACT
CTCTCCTCAGAGAAGTTACTGGTTGCTTTCAGAATGTCAGCGTATGTGAAAGTTGATTTGTCTAAGCGAATGACC
TTGATTTTTCTGATAGCCATGGCGATGATCCACCTGAACTGGAAGTCATGTCATGTCTGGTTTTCGACCCATCT
AAGAGATCGATTTCTGCTTCCCTTGAAGCCTTAACAACCATAAGTGTACAATACCTGATACCACTAAACATGCAA
TAAACGCCAATGCAAGAGCCAAGGAAATCCAAATCAAAGAAGAGTTCTTGGCCTGTTTCCCTAGGACTTGGTTGG
AAATCTTCCCTCGTGTGTTCCCTGATAAGGGCGAATTCGCGGCCGCTAAATTCAATTTCGCCCTATAGTGAGTCGT
ATTACAATTCCTACTGGCCGTCGTTTTAC
```

T7 promoter

